

OS

METABOLISM DEPARTMENT
AGRICULTURAL DIVISION
CIBA-GEIGY CORPORATION
GREENSBORO, NORTH CAROLINA

CHARACTERIZATION AND IDENTIFICATION OF MAJOR
TRIAZOLE-¹⁴C AND
PHENYL-¹⁴C CGA-169374 METABOLITES IN RATS

Registration Category: Pesticide Assessment Guidelines
Section 85-1
Low Dose
High Dose
Preconditioned Low Dose

Study No: M16-420-29A, 30A, 31A, 33A
M16-420-26A, 27A, 28A, 32A

Report No.: ABR-90019 Project No.: 420988

Study Approved
Director: Thomas M. Capps By: Darrell Sumner
Title: Senior Group Leader, Title: Manager,
Animal Metabolism Animal Metabolism

Signature: *Thomas M. Capps* Signature: *D. Sumner*
Date: 9/13/90 Approval Date: 9/13/90

Submitted by: H. P. Barr and T. J. Carlin

Sponsor: CIBA-GEIGY Corporation
Agricultural Division
Metabolism Department
410 Swing Road
P.O. Box 18300
Greensboro, NC 27419

Testing Period (Analytical Phase II): 9/19/88 - 6/14/90

TABLE OF CONTENTS

	<u>PAGE NO.</u>
GLP COMPLIANCE STATEMENT.....	5
QUALITY ASSURANCE STATEMENT.....	6
GENERAL INFORMATION.....	7
I. INTRODUCTION.....	8
II. SUMMARY.....	8
III. MATERIALS AND METHODS.....	9
IV. CIRCUMSTANCES AFFECTING THE STUDY.....	18
V. RESULTS AND DISCUSSION.....	18
VI. CONCLUSIONS.....	27
VII. LIST OF TABLES	
TABLE I. BALANCE DATA SUMMARY FROM ABR-88043.....	28
TABLE II. FECAL EXTRACTABILITY.....	29
TABLE III. PERCENT DISTRIBUTION OF MAJOR FECAL METABOLITES FROM HPLC PROFILE.....	30
TABLE IV. LIVER EXTRACTION ^{14}C BREAKDOWN (POOLED, HIGH DOSE, PHENYL, MALE).....	31
TABLE V. ELEMENTAL ASSIGNMENTS FOR THE MAJOR IONS IN THE EI SPECTRUM OF METABOLITE A BASED ON ACCURATE MASS MEASUREMENT.....	32
TABLE VI. CHROMATOGRAPHIC RETENTION TIMES OF METHOXYLATED CGA-169374 (DIASTEREOMERIC PAIRS) AND METHOXYLATED CGA-205375 STANDARDS COMPARED TO METHYLATED METABOLITE A AND B ISOMERS.....	33

TABLE OF CONTENTS (Continued)

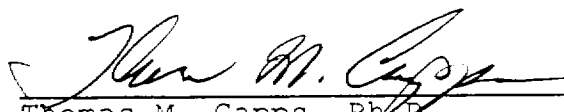
	<u>PAGE NO.</u>
VIII. LIST OF FIGURES	
FIGURE 1. CHEMICAL NAMES AND STRUCTURES.	34
FIGURE 2. HPLC PROFILE COMPARISON OF HIGH DOSE, FEMALE, FECES EXTRACTS.....	37
FIGURE 3. HPLC COMPARISON OF HIGH DOSE, FEMALE, RAW URINE.....	38
FIGURE 4. NORMAL PHASE HPLC CO- CHROMATOGRAPHY OF METABOLITE C AND CGA-205375 STANDARD.....	39
FIGURE 5. COMPARISON OF EI SPECTRA FOR METABOLITE C AND CGA-205375 STANDARD.....	40
FIGURE 6. METHANE CI SPECTRUM OF METABOLITE C.....	41
FIGURE 7. 2D-TLC CO-CHROMATOGRAPHY OF THE MAJOR URINARY METABOLITE OF TRIAZOLE- ¹⁴ C-CGA-169374 WITH CGA-71019 STANDARD.....	42
FIGURE 8. HPLC CO-CHROMATOGRAPHY OF A LIVER ISOLATE WITH CGA-189138 STANDARD.....	43
FIGURE 9. COMPARISON OF EI MASS SPECTRA OF THE LIVER METABOLITE AND CGA-189138 STANDARD.....	44
FIGURE 10. REPRESENTATIVE HPLC CHROMATOGRAM AND HISTOGRAM FROM THE MULTIPLE INJECTION ISOLATION OF METABOLITES A, B, AND C FROM FECES EXTRACT.....	45
FIGURE 11. FLOW DIAGRAM FOR THE ISOLATION AND PURIFICATION OF FECAL METABOLITES.....	46
FIGURE 12. COMPARISON OF THE EI AND CI MASS SPECTRA OF METABOLITE A..	47

TABLE OF CONTENTS (Continued)

	<u>PAGE NO.</u>
VIII. LIST OF FIGURES (Continued)	
FIGURE 13. COMPARISON OF THE EI SPECTRA OF METABOLITE A AND CGA-205375 STANDARD SHOWING A SHIFT EFFECT.....	48
FIGURE 14. COMPARISON OF THE EI AND CI MASS SPECTRA OF METABOLITE B..	49
FIGURE 15. COMPARISON OF THE EI MASS SPECTRA OF METABOLITE B AND CGA-169374 SHOWING A SHIFT EFFECT.....	50
FIGURE 16. FAB SPECTRUM OF METABOLITE B..	51
FIGURE 17. COMPARISON OF THE EI MASS SPECTRA OF THE PAIRS OF ISOMERS OF METABOLITES A AND B.....	52
FIGURE 18. COMPARISON OF THE AROMATIC REGIONS OF THE PROTON NMR SPECTRA OF METABOLITE B2 AND ONE DIASTEREOMER OF CGA-169374.....	53
FIGURE 19. AROMATIC REGION OF A DIFFERENCE NOE PROTON NMR SPECTRUM OF METABOLITE B1 OBTAINED WITH IRRADIATION AT 6.79 PPM.....	54
FIGURE 20. COMPARISON OF MASS SPECTRA OF METABOLITE B1 WITH ORTHO AND META METHOXY CGA-169374 STANDARDS.....	55
FIGURE 21. PLAUSIBLE MECHANISM FOR FORMATION OF UNEXPECTED METABOLITE STRUCTURES BY THE NIH SHIFT.....	56
FIGURE 22. PROPOSED PATHWAY FOR THE METABOLISM OF CGA-169374 IN THE RAT.....	57
IX. ACKNOWLEDGEMENT.....	58
X. REFERENCES.....	58

GLP COMPLIANCE STATEMENT

The majority of the metabolite characterization and identification phase of this study was conducted prior to October of 1989 and was conducted in accordance with good and acceptable scientific practices. The work conducted after October 1989 and preparation of the final report were completed in accordance with EPA Good Laboratory Practice Standards - 40 CFR 160.



Thomas M. Capps, Ph.D.
Study Director

Date 9/13/90

QUALITY ASSURANCE STATEMENT

Study Title: "Characterization and Identification of Major
Triazole-¹⁴C and Phenyl-¹⁴C CGA-169374
Metabolites in Rats"

Study Director: T. Capps

Protocol Numbers: 98-86 and 99-86

Final Report Number: ABR-90019

Pursuant to Good Laboratory Practice Regulations, this statement verifies that the aforementioned study was inspected and/or audited and the findings reported to CIBA-GEIGY Management and to the Study Director by the Quality Assurance Unit on the dates listed below.

<u>AUDIT TYPE</u>	<u>INSPECTION/AUDIT DATE/S</u>	<u>REPORTING DATE</u>
Final Report	March 13-16, 1990 June 28, July 03, 1990	March 19, 1990 July 03, 1990

Prepared By: Jeffrey A. Hull
Date: 24 Aug 90

GENERAL INFORMATION

Study Participants P. Barr, T. Carlin, W. Meadows

Test Material: CIBA-GEIGY Designation:
CGA-169374, 1-[2-[4-(4-chloro-
phenoxy)-2-chlorophenyl-
(4-methyl-1,3-dioxolan-2-yl)-
methyl]]-1H-1,2,4-triazole

Testing Facilities: Biological Phase
WIL Research Laboratories, Inc.
Ashland, OH 44805-9281

Analytical Phases I and II
CIBA-GEIGY Corporation
Agricultural Division
Metabolism Department
410 Swing Road
P.O. Box 18300
Greensboro, NC 27419

Study Initiation: December 4, 1986

Study Completion: September 13, 1990

Protocol Numbers: 98-86 (Phenyl) and Amendments
99-86 (Triazole) and Amendments

Archives: Protocols, raw biological data and
two biological reports (WIL-82013
and WIL-82014) are filed and
archived at WIL Research
Laboratories, Inc., Ashland, OH.

A copy of the protocols, raw data
for Analytical Phase I and Phase
II, and these reports are filed and
archived at Metabolism Residue
Chemistry, L-Building, CIBA-GEIGY
Corporation, Greensboro, NC. The
specimens related to these reports
are stored in the Metabolism
Residue Freezer, CIBA-GEIGY
Corporation, Greensboro, NC.

INTRODUCTION

CGA-169374, 1-[2-[4-(4-chlorophenoxy)-2-chlorophenyl-(4-methyl-1,3-dioxolan-2-yl)-methyl]]-1H-1,2,4-triazole, is a new fungicide being developed by CIBA-GEIGY. The structures of this compound and its metabolites are shown in Figure 1. The objective of this study was to isolate and identify the significant metabolites found in the feces and urine from rats when the compound was dosed according to a FIFRA protocol.

SUMMARY

The samples for this project originated from studies involving the test substance labeled on the phenyl² and triazole³ rings. The balance data for both labels was summarized in ABR-88043¹ and showed that >98% of ¹⁴C in all cases was excreted with >78% in all cases eliminated in the feces. Also, 50% of the ¹⁴C excreted in the feces was eliminated within 24 hours for low dose groups and by 48 hours for high dose groups. Individual urine and feces samples, either day 2 or day 3, were chosen from male and female rats for high, low, and preconditioned dose rates to profile for characterization and selection of metabolites for isolation and identification. Metabolite profiles were obtained by radio-HPLC analysis of raw urine and feces extracts. These profile data were analyzed to determine common metabolites between dose levels, sexes, and substrates and their respective abundances.

Since between 78 and 95 % of ¹⁴C was excreted in the feces, the primary focus was centered on the characterization and identification of fecal metabolites. The major metabolites isolated from feces were referred to as A, B, and C in order of their elution on reverse phase HPLC systems used in profiling the fecal extracts. The three combined accounted for an average of 68.6% of dose and metabolite C was only observed at high dose levels. The three major metabolites were isolated from fecal samples chosen from high dose level day 2 and day 3 phenyl labeled female feces which were combined and extracted. Various spectral analyses were obtained on the fecal metabolites. These data support the assignment of metabolite A as hydroxy-CGA-205375, metabolite B as hydroxy-CGA-169374, and metabolite C as CGA-205375. Metabolite A and B each separated into two isomers by

normal phase HPLC. For each metabolite the individual isomers, A1 and A2 for example, gave identical mass spectra. Proton NMR indicated that for each hydroxy isomer of A and B the site of substitution was on the outer phenyl ring. Difference NOE experiments provided some evidence that the most abundant isomer of hydroxy-CGA-169374 was not substituted ortho to oxygen on the outer ring. The specific sites of substitution were determined by comparison to prepared standards (see Figure 1) and provide evidence for the occurrence of an unexpected rearrangement of chloride, analogous to the NIH shift mechanism.

The metabolite distribution was more complex in urine than in feces, with greater variability resulting from label difference. Based on the balance data and individual urine profiles, no single urinary metabolite exceeded 10% of elimination, so that minimal metabolite identification was attempted. A single urinary metabolite, found distinctly in the triazole dosed rat urine, was isolated and identified as CGA-71019, triazole, by TLC and HPLC co-chromatography. This urinary metabolite represented the only significant example of cleavage of the alkyl bridge between the ring systems.

One tissue metabolite was isolated and characterized from pooled high dose, phenyl labeled liver samples. This metabolite was shown to be CGA-189138 by two dimensional TLC co-chromatography, reverse phase HPLC co-chromatography, and mass spectral analysis.

MATERIALS AND METHODS

Dose Material: The test compound consisted of ¹⁴C-CGA-169374 labeled either in a phenyl or triazole ring, as well as a cold standard for preconditioning. The lot numbers, specific activities, and radiochemical purities of the test compound are listed in the Analytical Phase I report¹. The dose levels were 300 mg/kg for high dose and 0.5 mg/kg for low dose.

The stability of the labeled and preconditioning dosing solutions was verified by HPLC analyses at WIL Research Laboratories during the in-life phase of the study^{2,3}.

Test Materials: Samples for characterization were chosen from a set of rat urine, feces, and tissue

samples as described in ABR-88043¹. These samples had been obtained from WIL Research Laboratories and were stored at freezer temperatures at CIBA-GEIGY.

Although the time duration from the conclusion of the Biological phase and the completion of Analytical phase II consisted of approximately 30 months, there was no indication of problems with metabolite stability. All specimens and isolates were stored at freezer temperature, when not under study. Re-analysis of both standards and isolated metabolites after long periods of storage showed no evidence of decomposition.

The following synthetic standards were used in this work: CGA-169374, S-85-0812, B43512, chemical purity 96.1%; CGA-205374, NV-XVII-66, B04352, chemical purity N/A; CGA-205375, NV-XVII-68, B04349, chemical purity N/A; CGA-189138, NV-XVII-70, B04350, chemical purity N/A; CGA-71019, chemical purity N/A, CGA-169374, Isomer 1 SG-III-39 (top), and Isomer 2 (Bottom) SG-III-39, chemical purity N/A. GB-XLIV-72 (GB-XLIV-56B), B05795, chemical purity 99%; GB-XLIV-73 (GB-XLIV-63A), B05796, chemical purity 99%; WRL-V-1-1, B05649, B05781, B05893, chemical purity 96.3%; WRL-IV-95, B05650, B05780, B05892, chemical purity 97.4%. MCO-III-58A, B05890, chemical purity 91.5%; MCO-III-58B, B05889, chemical purity 90.8%; WRL-V-33, B05891, chemical purity 97.7%; GB-XLV-17, B05874, chemical purity 98.8%; MCO-III-68, chemical purity N/A. The synthetic standard MCO-III-68 was used for chromatographic comparison prior to the compilation of the full synthesis characterization data package, which was completed shortly thereafter and before the study completion date. The standard used was an aliquot of the fully characterized lot which had been previously submitted for mass spectral analysis. This circumstance did not affect the integrity or outcome of the study. All standards were judged sufficiently pure for qualitative comparisons based on chromatographic and mass spectral analyses.

Radioassay Procedures: Radioassays were performed using a Beckman model 3801 liquid scintillation counter equipped with a "Chrom" package, which was used to produce histograms. Liquid samples and HPLC eluates were assayed directly in 15 ml of Ready Safe (Beckman) liquid scintillation cocktail. Combustion of homogenized liver subsamples was performed on a Harvey Oxidizer, Model OX400. The scintillation cocktail used for combusted samples was Oxosol-C14. DPM/g values were hand calculated.

Thin Layer Chromatography: Two dimensional TLC was performed on 20/20 cm precoated (250 micron) silica gel F-254 plates (Merck) in saturated chambers containing blotter paper. Some 500 and 1000 micron, F-254 plates (Analtech) were used for one and two dimensional TLC preparations of extracts. Systems used for 2D-TLC were:

TLC #1 toluene/chloroform/ethanol (1:1:1)

TLC #2 chloroform/methanol/formic acid/water (70:20:4:2)

The system used for one dimensional preparative TLC was TLC #1. Radioactive zones were detected using a Berthold model LB 292 Beta Camera and recorded on Polaroid 100 Land film. Visualization of standards was done under ultraviolet light and recorded on Polaroid 100 Land film. It was necessary to use an Iodine chamber for the visualization of the triazole, CGA-71019, standard. Extraction of silica gel of preparative TLC plates was accomplished by scraping the ^{14}C areas of interest into chloroform and extracting the silica gel using sonication and centrifugation.

Radio-High Performance Liquid Chromatography:

Radio-HPLC measurements were performed using two different units. Metabolite profiles were obtained on either instrument using the same solvent system. The units were:

UNIT 1: Perkin Elmer model 410 solvent delivery system
Perkin Elmer LC 95 UV detector at 240 nm
Raytest Ramona LS radioactive monitor
Foxy model 2200 fraction collector

UNIT 2: Spectra Physics SP 8700 solvent delivery system
SP 8750 solvent organizer
Perkin Elmer LC 75 UV detector with autocontroller at 240 nm
Berthold LB 503 HPLC radioactive monitor
Waters WISP model 710 autoinjector
(For Preparative HPLC)
Foxy model 2200 fraction collector

The conditions used for profiles and routine analysis were as follows:

For reverse phase profile:

System-A1

Column: Whatman Partisil 10 ODS 2 reverse phase analytical

Flow: 1 ml/min, for profiles, 0.6 min fractions were collected

Mobile Phase:

0-40 mins linear gradient, 100% water (0.025% phosphoric acid) to 100% acetonitrile
40-45 mins linear gradient, 100% acetonitrile to 100% methanol
45-50 mins 100% methanol
50-55 mins linear gradient, 100% methanol to 100% water (0.025% phosphoric acid)

For reverse phase preparative HPLC:

System-A2

Column: Whatman Magnum M9 Partisil ODS 2

Flow: 2 ml/min, 0.4 min fractions were collected starting at 22 min

Mobile Phase: same gradient as A1

For HPLC prep of the triazole urinary metabolite:

System-B

Column: Whatman Magnum M9 Partisil ODS 3

Flow: 2 ml/min, 0.4 min fractions were collected starting at 22 min

Mobile Phase: 100% water

For normal phase HPLC:

System-C analytical

Column: Whatman Partisil 10

Flow: 1 ml/min

Mobile Phase: 15% ethanol, 85% heptane

System-D preparative

Column: Whatman Magnum M9 Partisil 10

Flow: 2 ml/min, 0.4 min fractions were collected starting at 22 min

Mobile Phase: 20% ethanol, 80% heptane

The reverse phase HPLC system for the purification of the liver metabolite:

System-E

Column: Whatman Magnum M9 Partisil ODS 2

Flow: 2 ml/min, 0.5 min fractions were collected

Mobile Phase:

0-40 mins	linear gradient, 75% water (0.025% phosphoric acid), 25% acetonitrile to 100% acetonitrile
40-45 mins	linear gradient, 100% acetonitrile to 100% methanol
45-50 mins	100% methanol
50-55 mins	linear gradient, 100% methanol to 75% water (0.025% phosphoric acid), 25% acetonitrile

Profiling of Urines: Day 2 or 3 urine samples were chosen at random from one male and one female rat for each of the three dose rates and for each dose label. Profiling of raw urine was done using either HPLC unit #1 or #2 and using HPLC system A1.

Extraction of FIFRA rat feces for profiling: Five to six grams of each feces sample to be profiled was weighed and total dpms calculated for each respective sample. A sample from day 2 or day 3 was chosen from each sex and each label for the high, low and multidose rates making a total of 12 feces samples profiled. The samples were individually weighed into separate 125 ml Erlenmeyer flasks to which 50 ml of 9:1 acetonitrile: water was added. The sample was polytronized for five minutes, decanted, and the supernatant filtered through reive angel filter paper under vacuum in a buchner funnel. Care was taken to keep transfer of the residue to the filter funnel to a minimum. This process was repeated three times and the final time the entire

residue was transferred to the buchner funnel and washed with 5-10 mls of the 9:1 acetonitrile:water. The fecal extracts were transferred to a 250 ml graduated cylinder and from each 500 microliters were aliquoted in duplicate for ^{14}C assay. Extractability was determined from this assay. The fecal extracts were concentrated under vacuum rotary evaporation and transferred to 15 ml graduated centrifuge tube using methanol. These were the extracts used for obtaining metabolite profiles.

Profiling of Fecal Extracts: The fecal extracts described above were profiled using the same HPLC units and solvent systems that were used for the raw urines.

Bulk Fecal Extraction for Isolation of Metabolites: The total feces samples from day 2 and 3 of four high dose, phenyl labeled, female rats, F220, F218, F216, and F214 were individually weighed and combined. This sample was extracted with 9:1 acetonitrile:water, 300 ml, by shaking the sample for 48 hours, decanting and filtering. The extraction was repeated with shaking for several hours, followed by polytronizing the remaining residue for 5 minutes in 9:1 acetonitrile:water. These respective extracts were assayed for ^{14}C and the extractability calculated. This extract, after combining and concentration by vacuum rotary evaporation to cryness, was brought up in about 200 ml of water, transferred to a 500 ml separatory funnel, and then partitioned 3X with 200 ml of chloroform.

The organic fractions were combined and assayed for ^{14}C . The combined organic fraction after concentration was banded on several 1000 micron prep silica gel TLC plates and developed in TLC system #1. The broad ^{14}C band of interest was located on each plate using the Berthold Beta camera. This band from each plate was scraped, and then combined and extracted with 1:1 chloroform:methanol by sonication and centrifugation.

The TLC extract was concentrated, and the 3 major metabolites isolated by automated, overnight, reverse phase HPLC using unit #2 and system A2. An example of the HPLC trace of one of the multi-injections and the histogram from the aliquoting of the total prep can be seen on Figure 10. The collected fractions from multiple injections were aliquoted and the peaks located by scintillation counting. The individual metabolite fractions were combined and assayed for ^{14}C .

The individual metabolite peaks were concentrated and spotted on 500 micron silica gel plates for a 2 dimensional prep using TLC systems #1 and #2. After development, the ¹⁴C spot of interest from each plate was scraped and extracted using chloroform and methanol by sonication and centrifugation. The integrity of these metabolite isolates was confirmed using the original HPLC system for profiling the extracts, i.e., HPLC unit #1 or #2 and system A1.

Extraction, Isolation, and Purification of the Liver Metabolite: The liver samples from the high dose, phenyl labeled, male rats were combined and mixed in a blender. They had been previously homogenized for combustion. The total sample was weighed and a dpm/gram value obtained by combustion. The sample was then extracted by polytroning three times using 250 ml of 9:1 acetonitrile:water. Following extraction and filtration the extract was stripped of solvent by rotary evaporation. This aqueous extract was then partitioned three times with hexane followed by a single chloroform partitioning. Data on the extraction of liver may be seen in Table IV. Isolation of the liver metabolite was accomplished using HPLC unit #2 and system E to purify the hexane soluble fraction of the liver extraction which accounted for 56% of the starting ¹⁴C material in the combined liver sample. This metabolite isolate was compared to an authentic CGA-189138 standard by co-chromatography on the two dimensional TLC system #1 and #2, and reverse phase HPLC system #2, and solvent system A1. The isolated liver metabolite was further purified using 2D-TLC with systems #1 and #2 on a 500 micron prep plate. The area of interest was located using a Berthold beta camera, scraped, and the silica gel extracted using sonication in chloroform and centrifugation.

Isolation, Purification, and Characterization of the Triazole ¹⁴C Urinary Metabolite: The major metabolite in the high dose male triazole urine used for profiling was isolated using HPLC unit #2 and system B. Multiple, 150 μ l injections of filtered raw urine were made and 72, 0.2 minute fractions were collected for each injection. The ¹⁴C area of interest was located by liquid scintillation counting of aliquots of each fraction and these vials were combined and concentrated. The identity of the metabolite was determined by 2D-TLC co-chromatography with CGA-71019 using solvent systems #1 and #2. HPLC co-chromatography was conducted using HPLC unit #2 and system A1.

Mass Spectrometry: All mass spectral data were obtained on a VG 70-250 SQ double focusing mass spectrometer with an integrated VG 11-250J data system. For EI spectra, an ionizing energy of 70eV and a source temperature of 200°C were used. Methane was used as the CI reagent gas, with an ionizing energy of 200 ev and a source temperature between 175 and 200°C. Reagent gas pressure was adjusted by optimizing the mass 113:112 ratio for chlorobenzene. In both EI and CI, the magnet was calibrated using PFK in EI mode and the samples were introduced using a heated, direct insertion probe. FAB spectra were obtained in Magic Bullet (5:1 dithiothreitol:dithioerythritol) matrix, using a primary xenon atom beam at 8 kV and 1 amp current. Accurate mass data were obtained at 10,000 resolution, using PFK as the mass reference. High resolution EI data were obtained in scanning mode, while CI data were obtained from a narrow range voltage scan.

Nuclear Magnetic Resonance: Proton NMR Spectra of unknown metabolites were obtained on a Varian XL 200 NMR operated using standard parameters. Samples were dissolved in either deuteriochloroform or perdeuteromethanol. Difference NOE experiments were performed on a Varian XL 400 NMR. Experimental parameters were adjusted carefully by an experienced operator.

Methylation of Metabolites: Aliquots of the individual isomers of Metabolites A and B were taken to dryness and derivatized with 1 ml of ethereal diazomethane and 50 μ l of methanol for two hours at 60°C. The methylated metabolites were taken to dryness and dissolved in either methanol or toluene for chromatographic comparison to synthetic standard.

Gas Chromatography: Qualitative GC experiments were performed on an HP-5890 GC equipped with an NPD detector.

Column: 3 M DB-WAX capillary
Injector temperature: 240°C
Detector temperature: 220°C
Initial temperature: 220°C hold for one minute
Rate: 5°/min
Final temperature: 250°C
Final time: 10 min
Injection: ca. 200 ng in several μ ls, splitless

CALCULATIONS:

1. For dpm:

$$dpm = \frac{cpm - bkg}{efficiency}$$

2. For total radioactivity in a fraction

$$dpm = avg. dpm \times \frac{\text{Total volume}}{\text{Volume assayed}}$$

3. For percent recovery

$$\text{Percent Recovery} = \frac{\text{Total dpm in a fraction}}{\text{Total dpm in starting material}} \times 100$$

4. For the percent of total radioactivity for a specific metabolite in a fraction by HPLC.

$$dpm_{\text{vial}} = \frac{cpm_{\text{vial}} - cpm_{\text{Bkg}}}{\text{counter efficiency}}$$

$$\% \text{ radioactivity for a metabolite} = \frac{(\sum \text{dpm values in a chromatographic region})}{(\sum \text{dpm values in the histogram})} \times 100$$

5. For the total dpm in a solid by combustion:

$$\text{Total dpm} = dpm \times \frac{\text{Total weight}}{\text{Weight combusted} \times \text{combustion efficiency}}$$

6. For percent of dose of a specific metabolite based on HPLC.

$$\text{POD} = \frac{\% \text{ radioactivity in metabolite} \times \% \text{ radioactivity in fraction}}{100}$$

CIRCUMSTANCES AFFECTING THE STUDY

No circumstances occurred that adversely affected the integrity or outcome of the study.

RESULTS AND DISCUSSION

A detailed analysis of the ^{14}C accountability in rats dosed with triazole- ^{14}C -CGA-169374 and phenyl- ^{14}C -CGA-169374 was presented in ABR-88043¹. Table I is reproduced from that report and shows the balance data for both labels and the combinations of male/female and low, high, and preconditioned dose groups. These data indicate that greater than 98% of administered radioactivity was eliminated in feces and urine with the majority (greater than 78%) being eliminated in feces. Regardless of label or gender, elimination was rapid, with a half-life of ca. 24 to 48 hours depending on dose. Tissue deposition was low, representing 0.4-1.0 and 0.0-0.02 percent of dose for phenyl and triazole label, respectively.

The primary objective of this analytical phase II work was the identification of the significant metabolites of CGA-169374 formed in rats. Chromatographic metabolite characterization was carried out to target and identify the major metabolites, so that comparisons of metabolite patterns were also possible. Substrate pooling was only performed to provide sufficient metabolite mass for bulk isolation from feces and liver.

Feces and urine samples from either day two or three were chosen for characterization from individual male and female rats of each dose and label group. During these collection periods, radiolabeled compound elimination was still high, but changing less rapidly. It was expected that while the relative distribution of major metabolites might vary daily, their identity would not.

Chromatographic Characterization of Significant Metabolites

The majority of metabolites (greater than 78%) were eliminated in feces. Individual feces samples were

extracted with 9:1 acetonitrile:water prior to further characterization. Table II lists extractability data showing that recoveries were essentially quantitative. The fairly large scatter around 100% was a consequence of extracting small amounts of feces and using small aliquots. Extracts were profiled using reverse phase HPLC, and the column fractions were collected and counted to produce histogram representations of the major metabolites. Figure 2 compares the histograms from phenyl and triazole labeled, high dose, female feces. The three major chromatographic peaks correspond to the significant fecal metabolites and were designated as metabolites A, B, and C based on increasing retention time in HPLC. Table III lists the relative abundance of these metabolites broken down by dose level, label and gender. Metabolite C was observed mainly in high dose rats, while A and B are common to all dose groups. Some gender differences in the relative abundance of the fecal metabolites were observed, but in most cases the abundances are very similar when like samples of the different labels are compared. The later observation indicates that in the major fecal metabolites both ring systems are intact.

Total urinary elimination ranged from 8 to 22% of dose. Raw urine was profiled directly on HPLC system A1. The column recoveries ranged from 92 to 126% except for phenyl, low dose, male and phenyl, preconditioned dose, male and female which ranged from 64.6 to 69.3%. Metabolite profiles for urine were complex, with a greater variability between label, dose, and sex groups than was observed for the feces. The total urinary elimination as percent of dose is listed in Table I for all dose groups. Based on these values, and the assumption that the profile data of the chosen urine sample is representative of the profile of the total urinary elimination, no individual urine metabolites accounted for 10% or more of the total radioactivity.

As observed from Table I, the total percent of dose urinary elimination from phenyl and triazole labels are similar for all dose groups. Figure 3 compares HPLC profile of triazole and phenyl, high dose female urines, showing that the metabolic patterns are different for the two labels. The triazole labeled urines are distinctive in that they contain a major polar metabolite which accounts for between 21 and 70% of the labeled residue in the profiled urine samples. This predominant metabolite was not observed in phenyl labeled urines and was isolated and identified as

discussed below. The phenyl labeled urines showed in general a trend toward less polar metabolites and greater complexity in distribution than the triazole urines. Due to the low relative abundance of individual metabolites, in terms of percent of total elimination, and the variability among dose groups, no specific phenyl urinary metabolites were targeted for identification. Possible structures of these metabolites are discussed when the metabolic pathway is considered.

Isolation and Identification of Metabolites Which Match Existing Synthetic Standards

Fecal Metabolites A and B did not match any available standards by HPLC or TLC. The isolation and identification of these metabolites will be discussed in detail. Metabolite C from a bulk preparation was readily identified as CGA-205375 by chromatographic techniques. Figure 4 shows HPLC co-chromatography of Metabolite C with a synthetic standard of CGA-205375 in a normal phase HPLC system. The metabolite also co-chromatographed with the standard by 2D-TLC and reverse phase HPLC. The assignment of fecal Metabolite C was confirmed as CGA-205375 by comparing the EI spectrum of Metabolite C to the same spectrum of the synthetic standard as shown in Figure 5. Figure 6 shows the methane CI spectrum of Metabolite C which confirms the molecular weight.

The distinct triazole urinary metabolite was isolated from pooled high dose male urine by preparative HPLC. The purified metabolite was identified by 2D-TLC as triazole, CGA-71019, (Figure 7). Confirmation of the identity was obtained by HPLC.

Due to the low levels of tissue deposition in the rat, only very limited tissue analyses were performed. Liver was chosen as a representative tissue because, it exhibited comparable phenyl label distribution to other tissues, and was the only organ showing detectable triazole label residues. Table IV lists the distribution of radiolabeled material from the extraction steps of pooled, phenyl, high dose male liver. The majority, 56%, of the phenyl labeled residue partitioned into the hexane sub-fraction. This fraction was further purified by HPLC and 2D-TLC yielding an isolate which was identified as CGA-189138 (see Figure 1 for structure). The identity of this metabolite was confirmed by 2D-TLC co-chromatography, HPLC co-chromatography (Figure 8) and mass spectral

comparison to an authentic standard (Figure 9). This aromatic carboxylic acid has surprising organic solubility and appeared predominately in the hexane fraction. Mass spectral analysis showed that octadecanoic acid was a co-isolate, confirming the lipophilicity of the structure. The preference for tissue deposition of phenyl radio-label metabolites probably results from the high relative lipophilicity of the bridge cleaved phenyl metabolites. The bridge intact and cleaved triazole metabolites, being more polar, would have a preference for fecal and urinary elimination.

Isolation and Identification of Fecal Metabolites A and B

Since Metabolites A and B from feces did not match any available standards, it was necessary to isolate them for spectroscopic characterization. Due to the low specific activity of the high dosed rats (higher mass per dpm) and the even spread of the three major fecal metabolites seen in the female feces, the high dose female feces was chosen for bulk extraction. Also, because of the availability of standards and previous metabolism data on the phenyl ^{14}C labeled compounds associated with CGA-169374, the phenyl ^{14}C labeled samples were chosen. The day 2 and 3 feces samples for four rats were pooled and prepared by a multi-step procedure to isolate milligram quantities of Metabolites A, B, and C. Figure 10 shows an example of the HPLC data from a preparative HPLC run. The overall separation scheme as applied to feces is illustrated in a flow chart in Figure 11.

Gross Structure of A and B: Mass Spectral Analysis

Metabolites A and B from an initial bulk preparation were analyzed by several mass spectral techniques. The gross structure of these metabolites was readily determined by mass spectrometry in the manner described below.

Metabolite A: The methane CI and 70 eV EI spectra of Metabolite A are shown in Figure 12. The distinctive CI pseudomolecular ion pattern for methane of $(\text{M}+\text{H})^+$, $(\text{M}+29)^+$, and $(\text{M}+41)^+$ is observed at m/z 366, 394, and 406, respectively, and indicates that the nominal, monoisotopic molecular mass of the metabolite is 365. The presence of an abundant molecular ion at 365 is also observed in the EI spectrum. In both spectra a two

chlorine isotope pattern is observed. Figure 13 compares the EI spectrum of Metabolite A with the EI spectrum of CGA-205375. In the higher mass range the major masses for CGA-205375 are observed for Metabolite A as being shifted higher by 16 amu. This mass difference is readily assignable to the presence of an additional oxygen in the metabolite. Since the required probe temperature to volatilize Metabolite A was high (~300°C), the molecular weight was confirmed by observation of a m/z 366 peak in the FAB spectrum of this metabolite recorded in magic bullet at room temperature. The molecular formulas of the molecular ion and predominant fragment were determined by high resolution mass spectrometry in the scanning mode using EI. Assigned elemental compositions are listed in Table V.

Metabolite B: Parallel to the discussion of Metabolite A, the methane CI and EI spectra of Metabolite B are shown in Figure 14. Observation of m/z 422, 450, and 462 by CI indicates a nominal, monoisotopic molecular mass of 421 for Metabolite B. Comparison of the EI spectrum of Metabolite B with that of CGA-169374 (Figure 15) again shows the shift effect of the addition of oxygen on a non-fragmenting site in the molecule. The major fragments are loss of methylene-triazole (339 vs. 323) and loss of methylene-triazole and propylene oxide (281 vs. 265). A FAB spectrum obtained in magic bullet showed peaks at m/z 422, (M+H)⁺, and m/z 444, (M+Na)⁺ with two chlorine isotope clusters confirming the molecular weight assignment of Metabolite B (Figure 16).

Based on these mass spectral data, Metabolite A was assigned as hydroxy-CGA-205375 and Metabolite B as hydroxy-CGA-169374. The EI fragmentation showed the hydroxy substituent was associated with the diphenyl ether portion of the molecular, since the oxygen is retained on the ions which have lost the triazole or triazole and propylene oxide moieties. The lower mass fragmentation was nondescript and did not allow assignment of the hydroxy substitution to a specific phenyl ring.

Fine Structure of Metabolites A and B

As can be seen in Figure 1, the parent molecule has two chiral centers associated with the dioxolane ring substructure. As expected, CGA-169374 exists as two diastereometric pairs of enantiomers. The diastereomers can have different physical properties and for these molecules the diastereomers are separable by normal phase HPLC. When Metabolites A and B were further

characterized by normal phase HPLC, each metabolite separated into a pair of isomers which were indistinguishable by mass spectrometry. Figure 17 illustrates the similarity of the EI spectra for each pair of isomers. Based on the mass spectral analyses, it was possible to infer the nature of the Metabolites A and B as being hydroxylated on one of the phenyl rings. The fragmentation of the substituted biphenyl ether substructure was sufficiently nondescript so that the specific ring cannot be assigned. For A, hydroxy-CGA-205375, isomers from hydroxylation could involve either of the two phenyl rings and individual positions of substitution on each ring. For B, hydroxy-parent, isomers could involve the two phenyl rings, individual positions of substitution on a ring, and the diastereomers possible from the intact dioxolane moiety. Since the two pairs of isomers for Metabolites A and B were indistinguishable by mass spectrometry, bulk normal phase HPLC was used to prepare milligram quantities of each isomer for further structural characterization by NMR.

NMR Analyses of Pure Isomers

CGA-169374 and CGA-205375 had been previously studied by proton NMR at 200 MHz at CIBA-GEIGY central research, Ardsley, NY. The resonances for the diphenyl ether substructure had been assigned previously with the aid of a COSY experiment. The protons for each phenyl ring comprise a separate spin system. For CGA-205375 and both the diastereomers of CGA-169374, the outer disubstituted phenyl ring protons have the expected, classic AA'BB' 4 proton coupling pattern in an isolated spin system. For each of the four hydroxylated metabolites, resonances resulting from two trisubstituted phenyl spin systems are observed. An example is illustrated in Figure 18 showing the assignments for the hydroxy-parent metabolite B2 compared to a single diastereomer of CGA-169374. The resonances associated with the outer ring spin system are indicated. Similar comparison for all four metabolites clearly indicate that all the hydroxy metabolites are substituted on the outer phenyl ring, i.e., the ring where chlorine is para to the ether linkage. Apparently the deshielding effects of the chlorine and oxygen in this spin system are sufficiently similar so as to preclude the assignment of the site of hydroxylation on the outer ring.

Further attempts were made to characterize the position of substitution for these metabolite isomers by NMR experiments. A technique called difference NOE (Nuclear Overhauser Effect) subtracts proton spectra recorded

with and without irradiation of a selected proton resonance. The goal is to detect signals that are enhanced by transfer of magnetization through space to protons which are spatially close to the irradiated proton. It was speculated that protons ortho to oxygen on the outer ring would interact with the inner ring protons and conversely hydroxylation ortho to oxygen would eliminate that NOE enhancement. The metabolite isomer B1 was selected as the most likely candidate for this experiment, since it had the broadest dispersion of the aromatic resonances. Although the experiment failed on a 200 Mhz NMR, a successful experiment was performed at 400 Mhz. The difference NOE spectrum from irradiation of H_4 at 6.79 ppm is shown in Figure 19, along with the pair of structures the experiment was designed to differentiate. The enhancement at 7.06 ppm in the subtracted spectrum was interpreted as interaction between protons 4 and 9 as labeled in Figure 19. This result suggested that Metabolite B1 was hydroxylated ortho to chlorine on the outer phenyl ring. Other attempts at DNOE experiments to assign the remaining isomers failed. This type of experiment is very sensitive to sample preparation, instrumental parameters and spin physics. Due to the difficulties and possible ambiguities of complex NMR analyses on low levels of metabolites, comparison to synthetic standards was targeted as the best approach to unequivocally assigning the exact site of substitution.

Comparison of Metabolites A and B to New Synthetic Standards

Based on the preliminary fecal metabolite identification already discussed, synthetic standards were prepared for comparison. For synthetic considerations, standards of the methoxy equivalents of the speculated hydroxy-CGA-169374 were prepared. Individual diastereomers of the standard compounds methoxylated both ortho and meta to chlorine to the outer ring were prepared and characterized for use as standards. So that chromatographic comparison could be made, the diastereomers of Metabolite B were methylated with diazomethane.

Mass spectral analyses of methylated Metabolite B confirmed that a single methylation had occurred. Figure 20 shows a comparison of mass spectra of a single diastereomer of the substitutional isomer standards to Metabolite B1. Some subtle differences in the fragmentation patterns can be observed, but all three compounds have the same molecular weight (confirmed by CI) and gross structure, i.e., two chlorines and one methoxy group on the phenyl ether ring system.

Chromatographic comparison of the four expected standards (diastereomers of ortho and meta methoxy) and Metabolites B1 and B2 was carried out using both GC and normal phase HPLC. It was observed for the standards that GC was effective for resolving substitutional isomers, but in general diastereomers were found to co-elute under the GC conditions employed. Table VI lists the retention times of all the standards and metabolites for the LC and GC analyses. GC data clearly discriminated between the B metabolites and meta standards, while LC ruled out the ortho standards. The corresponding meta and ortho methoxy-CGA-205375 standards were prepared and compared chromatographically to methylated Metabolite A isomers. The ortho methoxy standard was found to match methylated A1, the less abundant A isomer. In summary, chromatographic comparison to standards of expected metabolites showed that the position of hydroxylation of Metabolites A2, B1, and B2 is neither ortho nor meta to chlorine on the outer ring.

These results were inconsistent with the mass spectral analyses which confirmed molecular weight and the gross structure and the NMR data which unequivocally indicated that the metabolites were substituted on the outer phenyl ring. A plausible explanation was proposed based on the NIH shift mechanism which has been invoked to explain intramolecular migrations during hydroxylation of aromatic compounds. The mechanism involves an epoxide intermediate, which in the case of Metabolites A and B, could open with a concomitant 1,2 chloride shift to produce a 3-chloro,4-hydroxy substitution pattern on the outer ring. A scheme for this mechanism is shown in Figure 21.

The occurrence of this shift was confirmed by preparation of the analogous three standards which, as shown in Table VI, matched Metabolites B1, B2, and A2. Note that all matches were confirmed by co-chromatography in both systems. Metabolite A1 is ortho hydroxy-CGA-205375 and Metabolite A2 is the corresponding 3-chloro,4-hydroxy isomer (structures summarized in Figure 1). Metabolites B1 and B2 correspond to the two diastereomers of the rearranged hydroxy-parent with a 3-chloro,4-hydroxy substitution pattern on the outer ring. These structures, still having a 1,3,4 substitution on the outer ring, are consistent with the splitting pattern observed for the outer ring spin system by proton NMR and with the D-NOE results since the 2 position would still be unsubstituted.

Precedence for a chloride shift by the NIH mechanism during metabolic hydroxylation of chlorinated phenoxy metabolites has been reported for 2,4-D and diclofop-Methyl⁴.

Metabolic Pathway

A proposed pathway for the metabolism of CGA-169374 in the rat is shown in Figure 22. The major process involves hydroxylation on the outer phenyl ring, producing either hydroxy-CGA-169374 or hydroxy-CGA-205375. The appearance of CGA-205375 only at high dose rates suggests that hydrolysis of the ketal may occur prior to hydroxylation and that the hydroxylation enzyme sites may be saturated at the higher dose level. Since no intermediate ketone, CGA-205374, is observed at a significant level, reduction of the ketal hydrolysis product occurs either rapidly or as a single step process forming CGA-205375 directly. In terms of the NIH shift mechanism in Figure 21, the Metabolites A1 and A2 would result from chloride retention and chloride shift, respectively. In contrast for Metabolite B, only disastereomers of the chloride shift substitution are observed and this structure may be favored due to steric effects of the dioxolane ring. This speculation would be consistent with the premise that cleavage of the dioxolane ring precedes hydroxylation in the formation of Metabolite A.

The preference for fecal elimination of the residues of CGA-169374 may be due in part to the relatively high molecular weight of these metabolites, ca. 366 and 422 for A and B. Biliary excretion is known to be an important route of elimination for compounds with molecular weights exceeding 300.

The observation of CGA-71019 in triazole labeled urine and CGA-189138 in liver provide evidence that some bridge cleavage is occurring. The structure of CGA-189318 and the surprising organo-solubility of this molecule help explain the preference for tissue deposition observed for the phenyl label. Apparently the bridge intact and cleaved triazole metabolites are sufficiently polar to be preferentially excreted in feces and urine. Although a dominant metabolite is not observed for the phenyl label rat urines, the urinary elimination is comparable for both labels. This observation requires the presence of additional minor

bridge cleaved phenyl metabolites. Structures related to CGA-189138 and its derivative are likely candidates for the additional urinary metabolites.

Hydroxylated metabolites have also been observed in specimens from goat and hen metabolism studies on CGA-169374, although not as the major metabolite^{5,6}. In both the hen and goat, CGA-205375 is the predominant metabolite. Significant amounts of conjugation were also observed for these test systems. Significant amounts of conjugates were not observed in rats, but might be present in minor amounts as unidentified urinary metabolites. Conjugates of hydroxy-CGA-169374 and hydroxy-CGA-205375 have been observed as major metabolites in plants⁷.

CONCLUSIONS

Fecal elimination dominates the disposition (78 to 95%) of both triazole and phenyl labeled ¹⁴C-CGA-169374 residues in the rat. All the significant metabolites (those which exceed 10% of dose) were eliminated in the feces and have been identified by mass spectrometry and NMR. The major Metabolites A and B are two isomers of hydroxy-CGA-205375 and two isomers of hydroxy-CGA-169374. The pairs of isomers accounted for an average 53.4 and 12.3 percent of dose, respectively. At the high dose level, Metabolite C, identified as CGA-205375, accounted for 12.6% of dose on average.

The urinary metabolite profiles were more complex than feces with greater variability among dose groups. Urinary elimination was a minor process and no individual urinary reached the 10% of dose level. A urinary metabolite, unique to the triazole label was identified as free triazole, CGA-71019.

A limited investigation of tissue residue in liver from the phenyl label identified, by mass spectrometry and co-chromatography, the major metabolite in liver as CGA-189138. The surprising organo-solubility of this carboxylic acid helps explain the preference for phenyl label tissue deposition which was observed previously.

The exact site of hydroxylation in the isomers of Metabolites A and B was determined by comparison to synthetic standards. These results provide evidence for a 1,2 chloride rearrangement, analogous to the NIH shift mechanism.

TABLE I. BALANCE DATA SUMMARY FROM ABR-88043

PHENYL-¹⁴C-CGA-169374

TRIAZOLOE-¹⁴C-CGA-169374

TABLE II. FECAL EXTRACTABILITY

Total Percent ^{14}C Recovery in Feces Extractions

<u>Label/Gender</u>	<u>Dose Level</u>		<u>Precondition</u>
	<u>High</u>	<u>Low</u>	
Triazole/Male	92	132	99
Triazole/Female	124	99.5	112
Phenyl/Male	109	117	79
Phenyl/Female	93	133	101

TABLE III. PERCENT DISTRIBUTION OF MAJOR FECAL METABOLITES FROM HPLC PROFILE

<u>Dose</u>	<u>Label</u>	<u>Gender</u>	<u>Percentage of Total Column Recovery</u> <u>(Percent of Dose Basis)</u>			<u>Sample</u>
			<u>A</u>	<u>B</u>	<u>C</u>	
Low	Triazole	M	73.44(62.92)	15.06(12.90)	-	F237
Low	Triazole	F	22.62(18.43)	22.35(18.21)	-	F236
Low	Phenyl	M	86.17(74.73)	1.81 (1.57)	-	F201
Low	Phenyl	F	76.46(66.2)	17.76(14.45)	-	F202
High	Triazole	M	81.09(71.77)	2.42 (2.14)	7.53 (6.66)	F251
High	Triazole	F	55.00(48.31)	18.17(15.95)	10.95 (9.62)	F250
High	Phenyl	M	82.99(78.52)	- (-)	11.16(10.16)	F213
High	Phenyl	F	36.03(30.75)	23.81(20.32)	28.34(24.19)	F214
Precond.	Triazole	M	65.85(51.58)	7.04 (5.51)	-	F257
Precond.	Triazole	F	55.92(46.18)	21.31(17.59)	-	F262
Precond.	Phenyl	M	72.46(51.20)	10.03 (7.92)	-	F223
Precond.	Phenyl	F	51.89(40.50)	23.95(18.69)	-	F232

TABLE IV. LIVER EXTRACTION ^{14}C BREAKDOWN (POOLED, HIGH DOSE, PHENYL, MALE)

<u>Fraction</u>	<u>^{14}C Material in Fraction</u>	<u>Percent of Starting Material</u>
Starting Material	86030	100
Extract		
Organic		
Hexane	47941	56
Chloroform	7317	9
Aqueous	9246	11
Residue	13267	15
	Total Recovery	91

TABLE V. ELEMENTAL ASSIGNMENTS FOR THE MAJOR IONS IN THE EI SPECTRUM OF METABOLITE A BASED ON ACCURATE MASS MEASUREMENT

<u>Nominal Mass</u>	<u>Elemental Composition</u>						<u>Observed Mass</u>	<u>Deviation (mmu)</u>
	¹² C	H	O	N	³⁵ Cl	³⁷ Cl		
367	16	13	3	3	1	1	367.0309	-0.5
365	16	13	3	3	2	0	365.0357	-0.7
285	13	9	3	0	1	1	284.9904	-0.5
283	13	9	3	0	2	0	282.9926	0.3

TABLE VI. CHROMATOGRAPHIC RETENTION TIMES OF METHOXYLATED CGA-169374 (DIASTEREOMERIC PAIRS) AND METHOXYLATED CGA-205375 STANDARDS COMPARED TO METHYLATED METABOLITE A AND B ISOMERS

	<u>Compound</u>	<u>Substit.^a</u>	<u>GC R.T.^b</u>	<u>LC R.T.^c</u>	<u>Match</u>
MeO-169374					
Isomers:	Metabolite B1 ^d		9.7	13.4	
	Metabolite B2 ^d		9.7	15.6	
	WRL-V-1-1	meta	7.7	12.0	
	WRL-IV-95	meta	7.7	13.8	
	GB-XLIV-72	ortho	9.4	13.4	
	GB-XLIV-73	ortho	9.4	11.8	
	MCO-III-58A	NIH Shift	9.7	13.4	B1 ^d
	MCO-III-58B	NIH Shift	9.7	15.6	B2 ^d
MeO-205375					
Isomers:	Metabolite A1 ^d		14.2	15.0	
	Metabolite A2 ^d		14.6	17.2	
	WRL-V-33	meta	11.1	15.2	
	GB-XLV-17	ortho	14.2	15.0	A1 ^d
	MCO-III-68	NIH Shift	14.6	17.2	A2 ^d

^aouter ring substitution (See Fig. 1, page 34)

meta = 2-MeO, 4-Cl

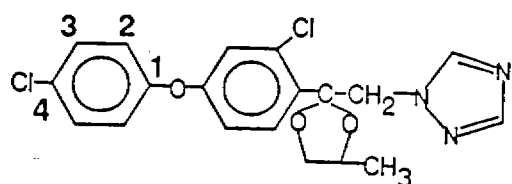
ortho = 3-MeO, 4-Cl

NIH Shift = 3-Cl, 4-MeO

^bGC retention time in minutes

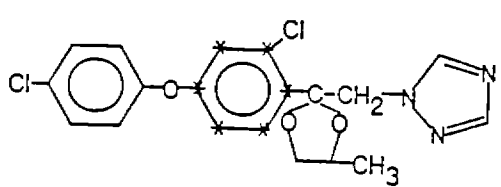
^cLC retention time in minutes, HPLC system C

^dmetabolites methylated for comparison to standards



1-[[2-[2-Chloro-4-(4-chlorophenoxy)phenyl]-4-methyl-1,3-dioxolan-2-yl]methyl]-1H-1,2,4-triazole

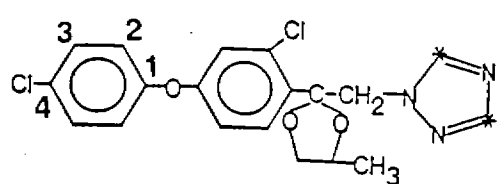
MW=406.27



D-¹⁴C-CGA-169374

1-[[2-[2-Chloro-4-(4-chlorophenoxy)-[U-ring-¹⁴C]-phenyl]-4-methyl-1,3-dioxolan-2-yl]methyl]-1H-1,2,4-triazole

MW=406.27

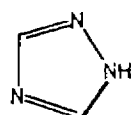


¹⁴C-CGA-169374

1-[[2-Chloro-4-(4-chlorophenoxy)phenyl]-4-methyl-1,3-dioxolan-2-yl]methyl]-1H-1,2,4-[3,5-¹⁴C]-triazole

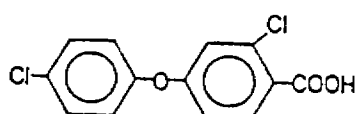
MW=406.27

FIGURE 1. CHEMICAL NAMES AND STRUCTURES



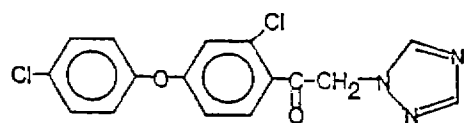
CGA-71019

Triazole
MW=69.07



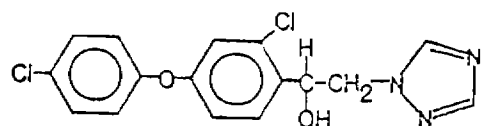
CGA-189138

MW=283.11



CGA-205374

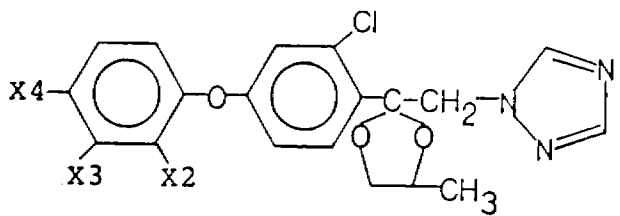
MW=348.19



CGA-205375 →

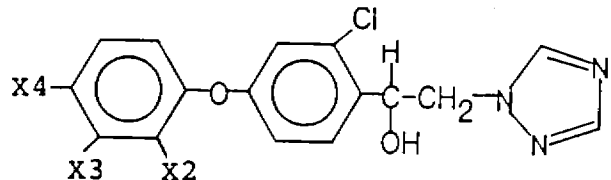
MW=350.21

FIGURE 1. CHEMICAL NAMES AND STRUCTURES (Continued)



Substitution

<u>X2</u>	<u>X3</u>	<u>X4</u>	<u>Compound</u>
H	H	Cl	CGA-169374 (2 diastereomers)
MeO	H	Cl	WRL-V-1-1 and WRL-IV-95 (diastereomers)
H	MeO	Cl	GB-XLIV-72 and -73 (diastereomers)
H	Cl	MeO	MCO-III-58A and -58B (diastereomers)
H	Cl	HO	Metabolite B1 and B2 (diastereomers)



Substitution

<u>X2</u>	<u>X3</u>	<u>X4</u>	<u>Compound</u>
H	H	Cl	CGA-205375
MeO	H	Cl	WRL-V-33
H	MeO	Cl	GB-XLIV-17
H	Cl	MeO	MCO-III-68
H	HO	Cl	Metabolite A1
H	Cl	HO	Metabolite A2

FIGURE 1. CHEMICAL NAMES AND STRUCTURES (Continued)

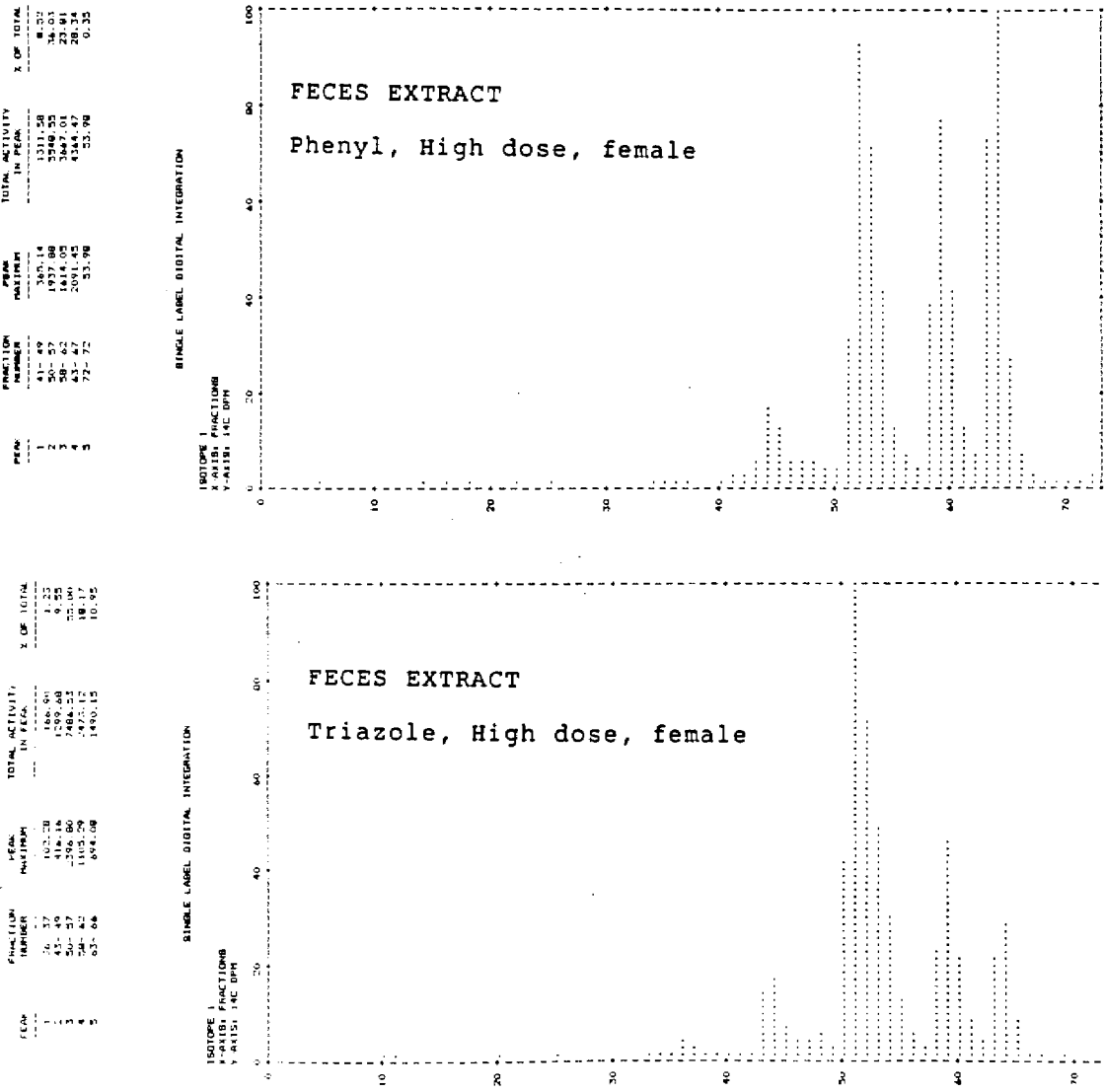


FIGURE 2. HPLC PROFILE COMPARISON OF HIGH DOSE, FEMALE, FECES EXTRACTS

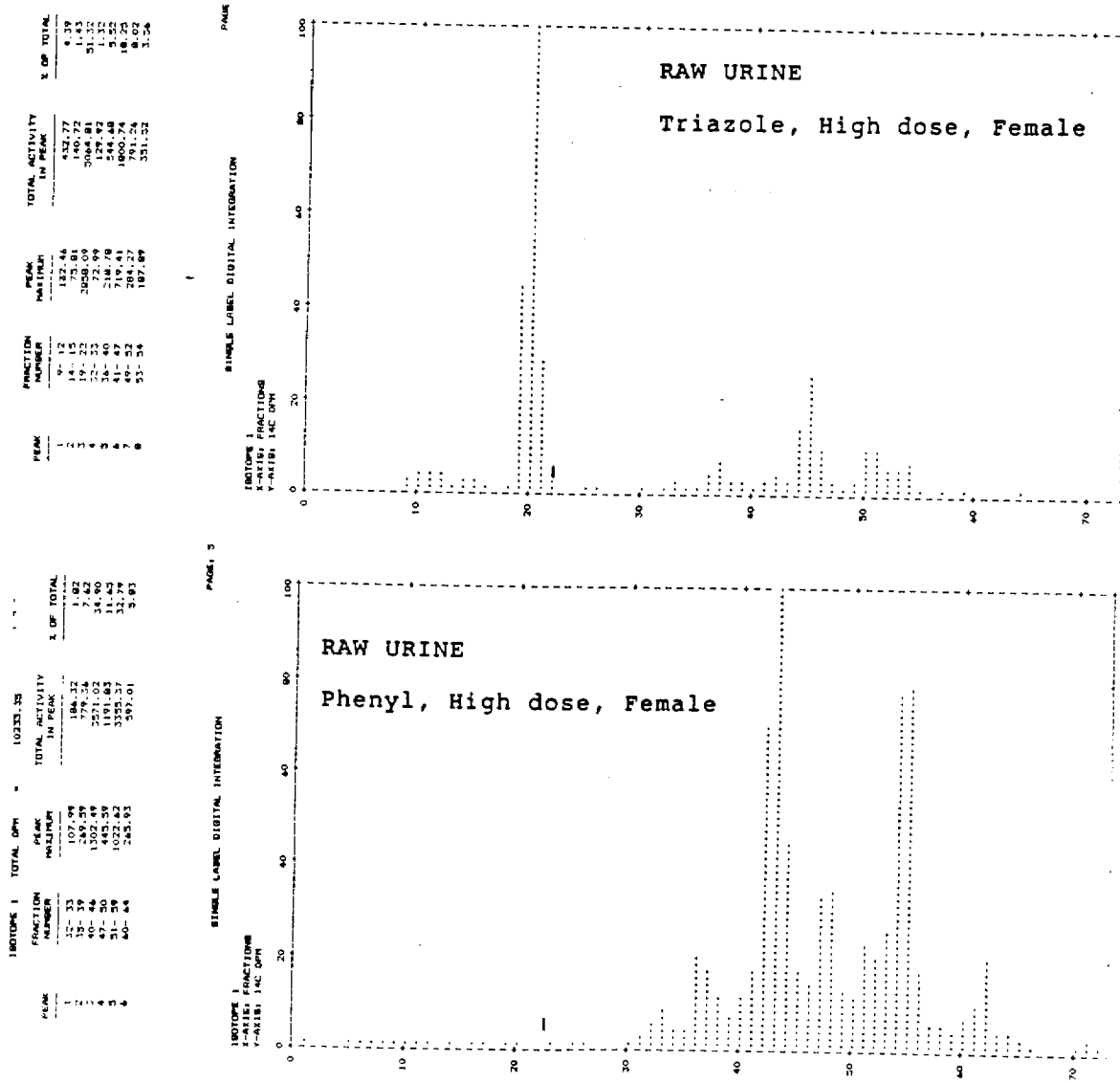


FIGURE 3. HPLC COMPARISON OF HIGH DOSE, FEMALE, RAW URINE

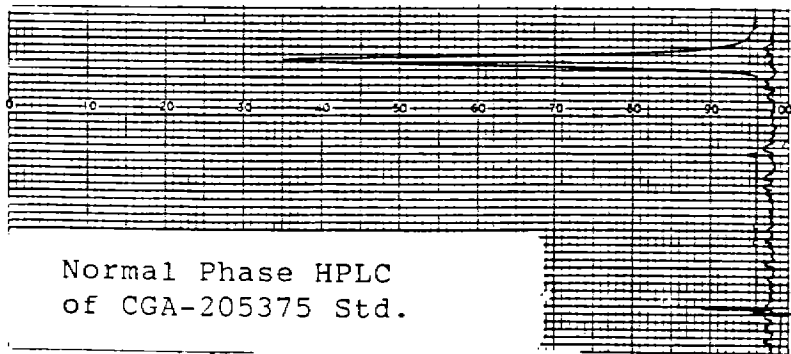
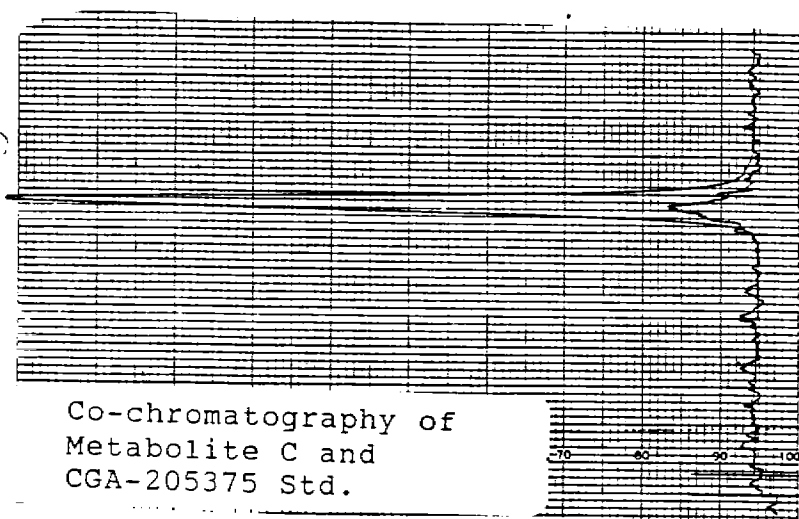


FIGURE 4. NORMAL PHASE HPLC CO-CHROMATOGRAPHY OF
METABOLITE C AND CGA-205375 STANDARD

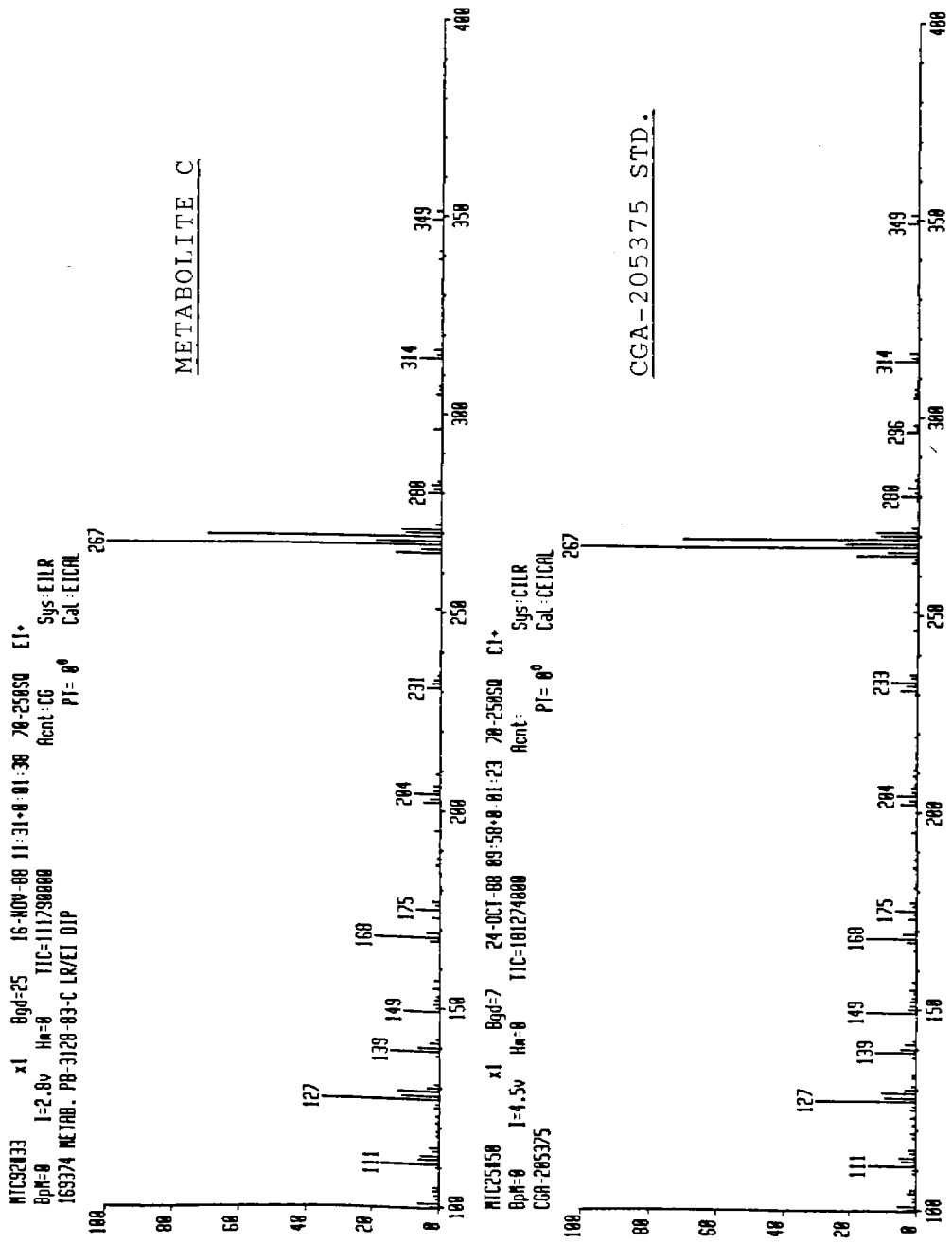


FIGURE 5. COMPARISON OF EI SPECTRA FOR METABOLITE C AND CGA-205375 STANDARD

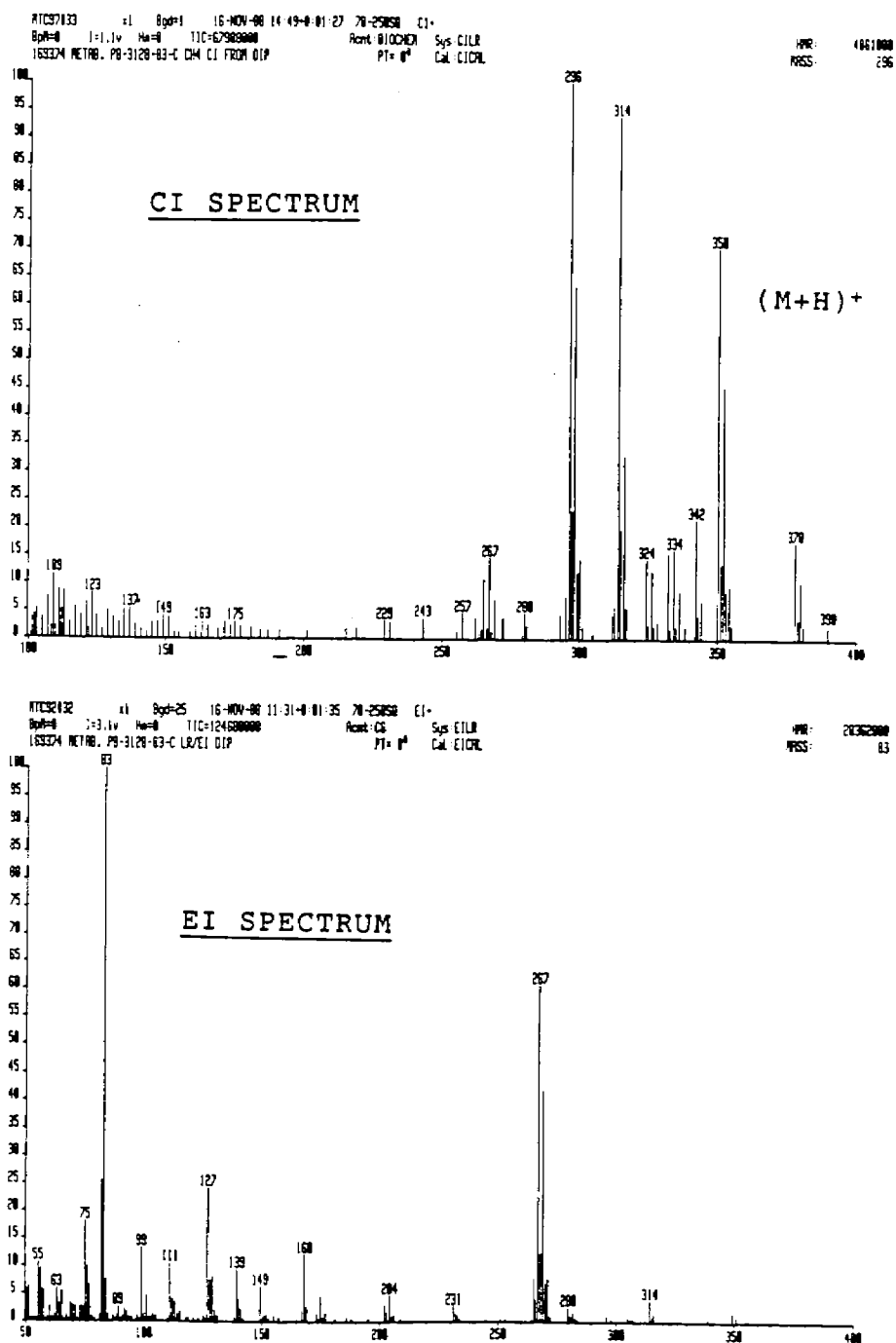
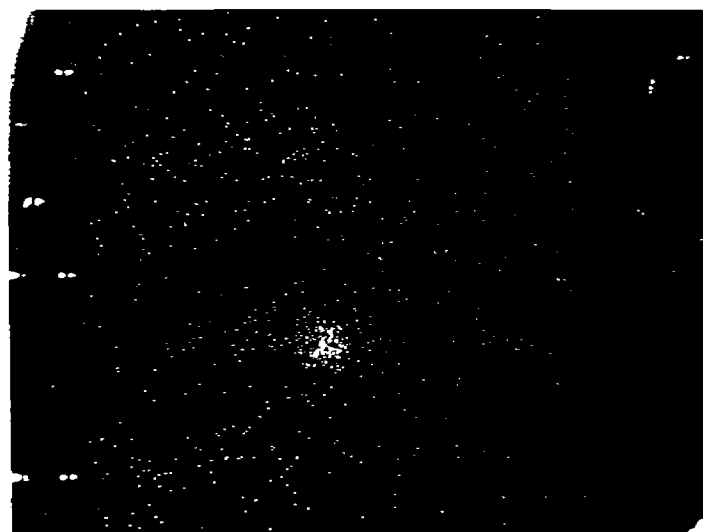
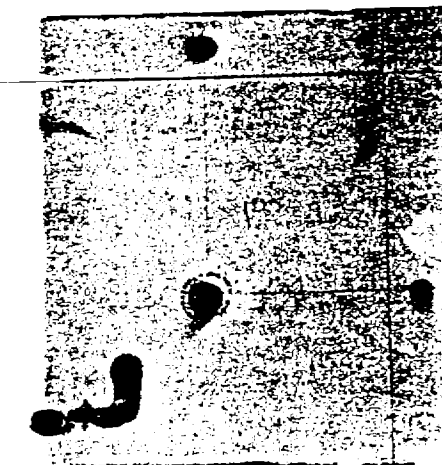


FIGURE 6. METHANE CI SPECTRUM OF METABOLITE C



BETA Camera
Picture



UV Picture

Standard at Origin
and in lanes:

CGA-71019

FIGURE 7. 2D-TLC CO-CHROMATOGRAPHY OF THE MAJOR URINARY
METABOLITE OF TRIAZOLE-¹⁴C-CGA-169374 WITH
CGA-71019 STANDARD

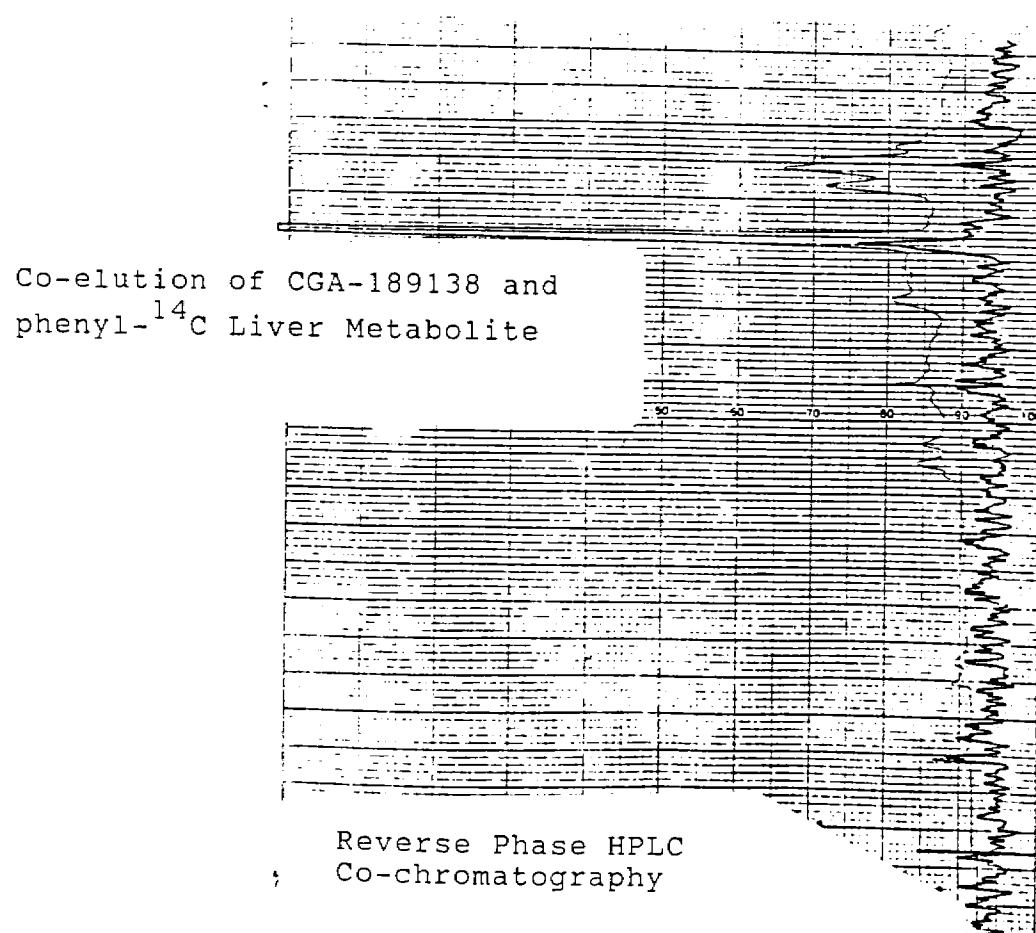


FIGURE 8. HPLC CO-CHROMATOGRAPHY OF A LIVER ISOLATE WITH CGA-189138 STANDARD

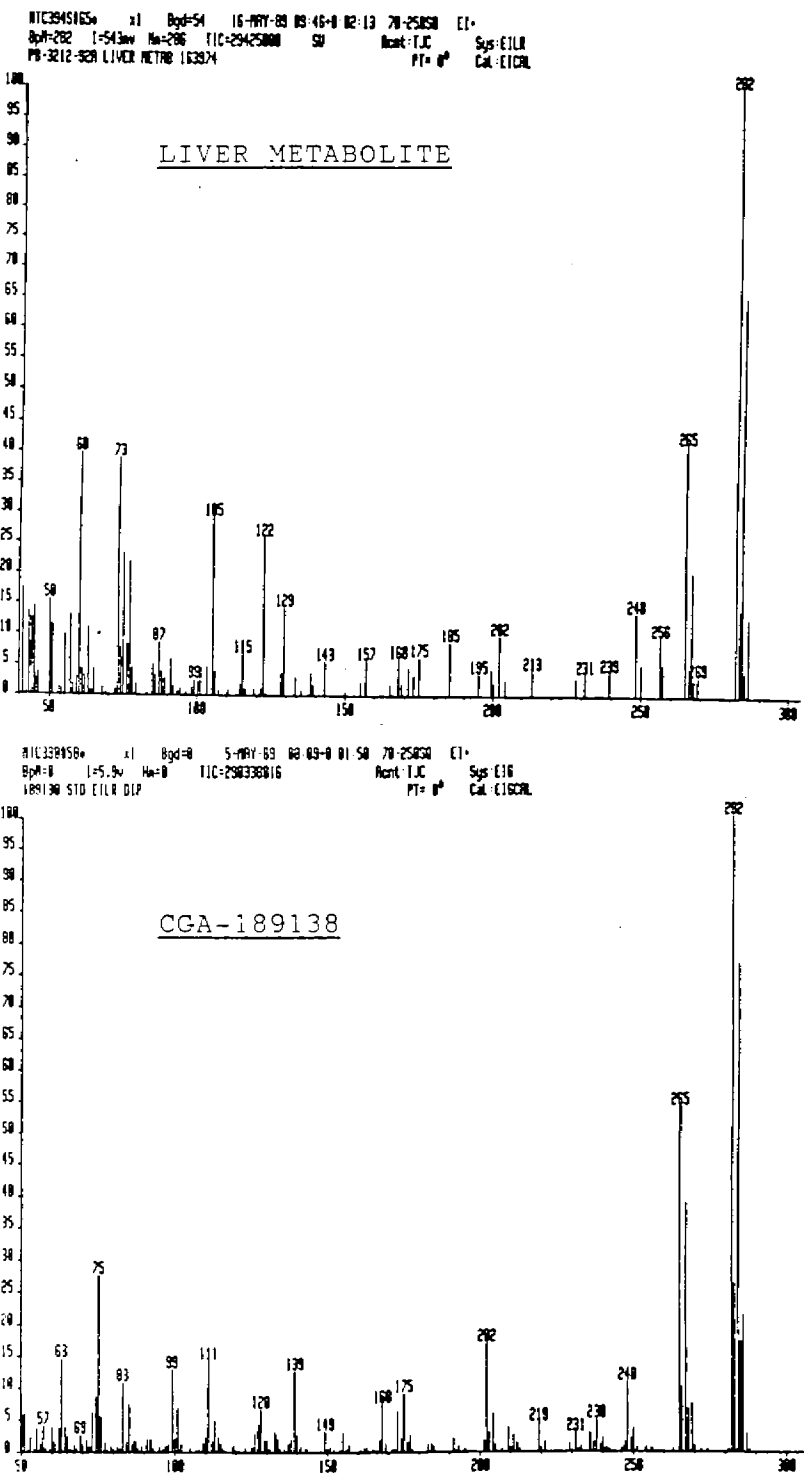


FIGURE 9. COMPARISON OF EI MASS SPECTRA OF THE LIVER METABOLITE AND CGA-189138 STANDARD

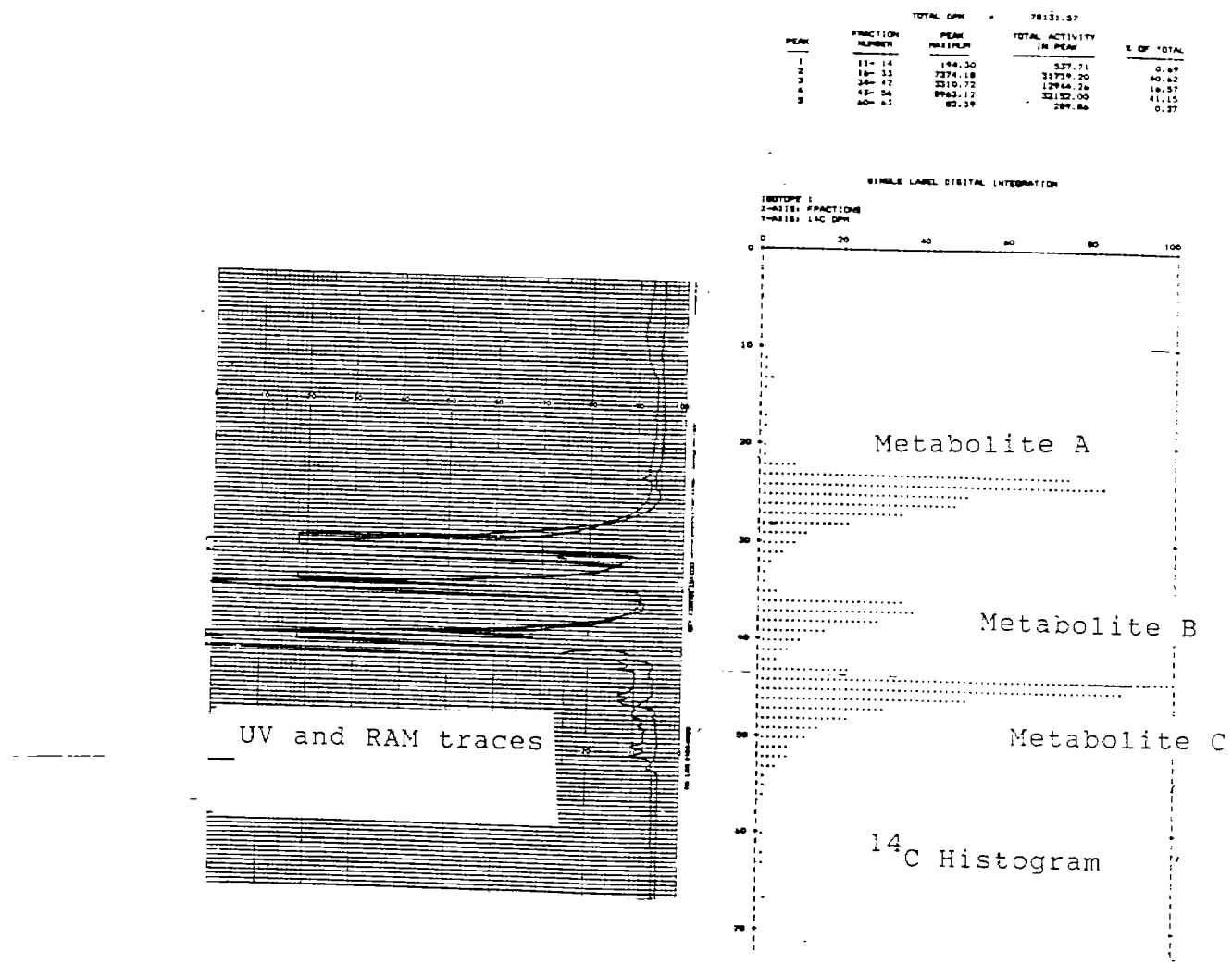


FIGURE 10. REPRESENTATIVE HPLC CHROMATOGRAM AND HISTOGRAM FROM THE MULTIPLE INJECTION ISOLATION OF METABOLITES A, B, AND C FROM FECES EXTRACT

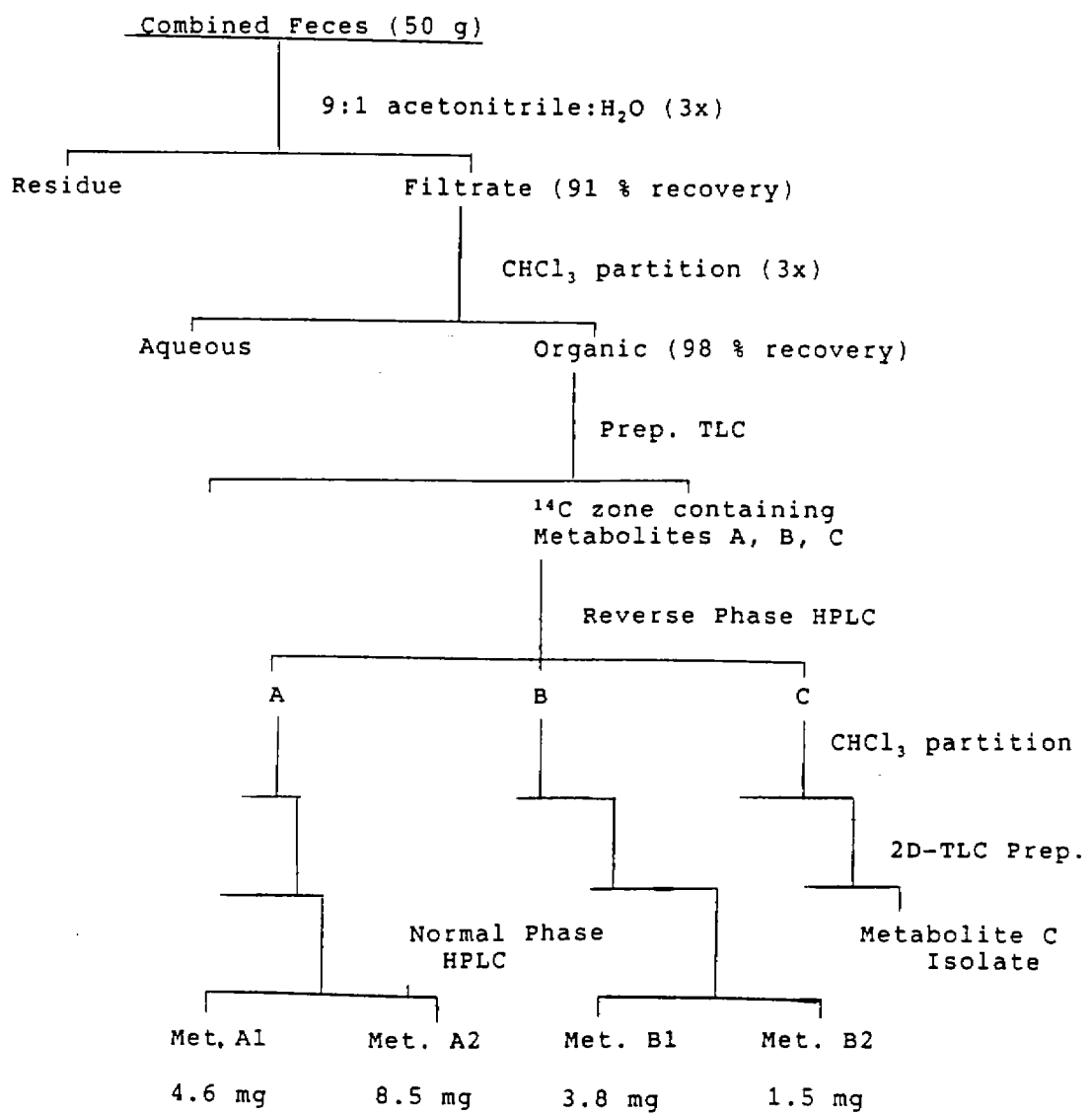


FIGURE 11. FLOW DIAGRAM FOR THE ISOLATION AND PURIFICATION OF FECAL METABOLITES

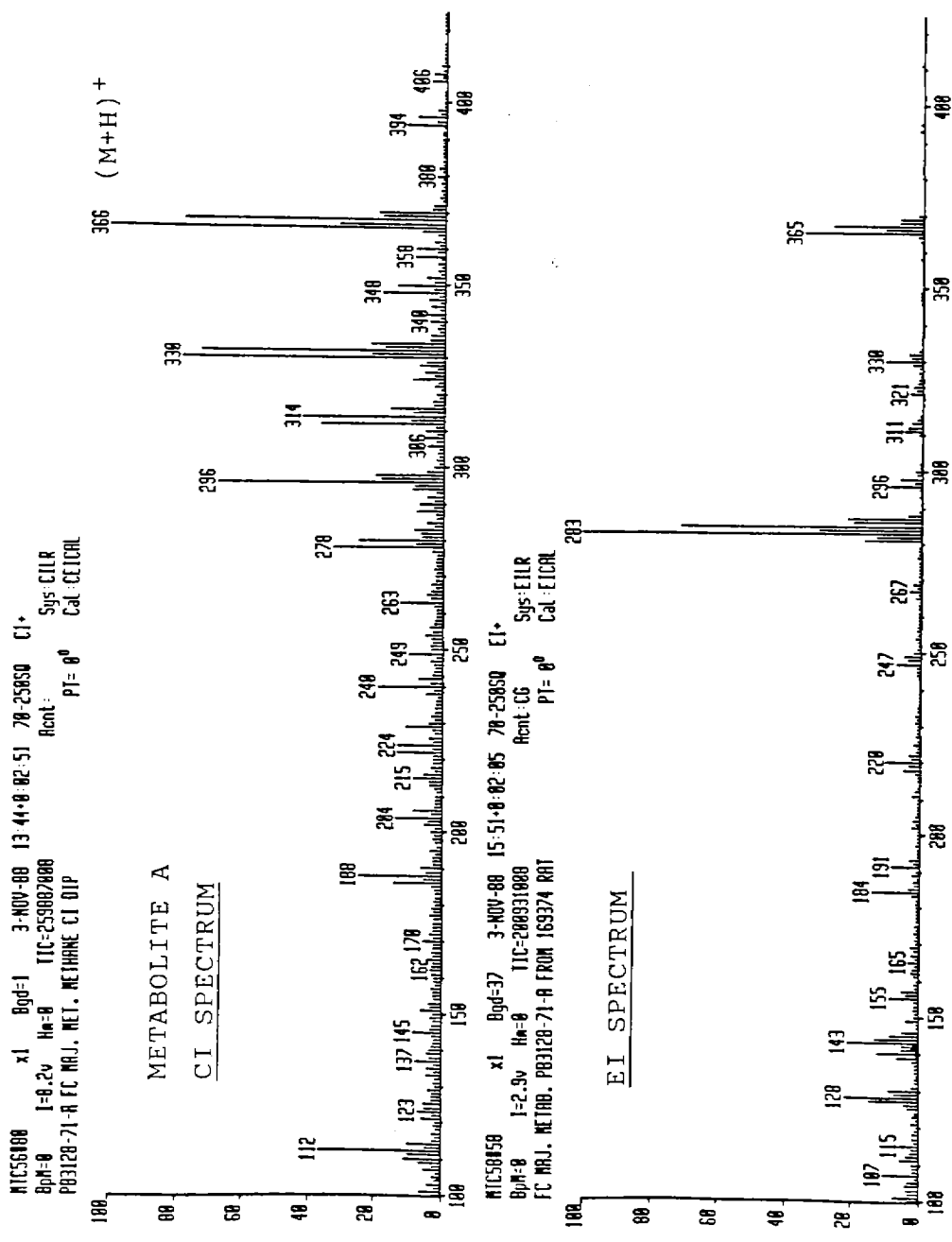


FIGURE 12. COMPARISON OF THE EI AND CI MASS SPECTRA OF METABOLITE A

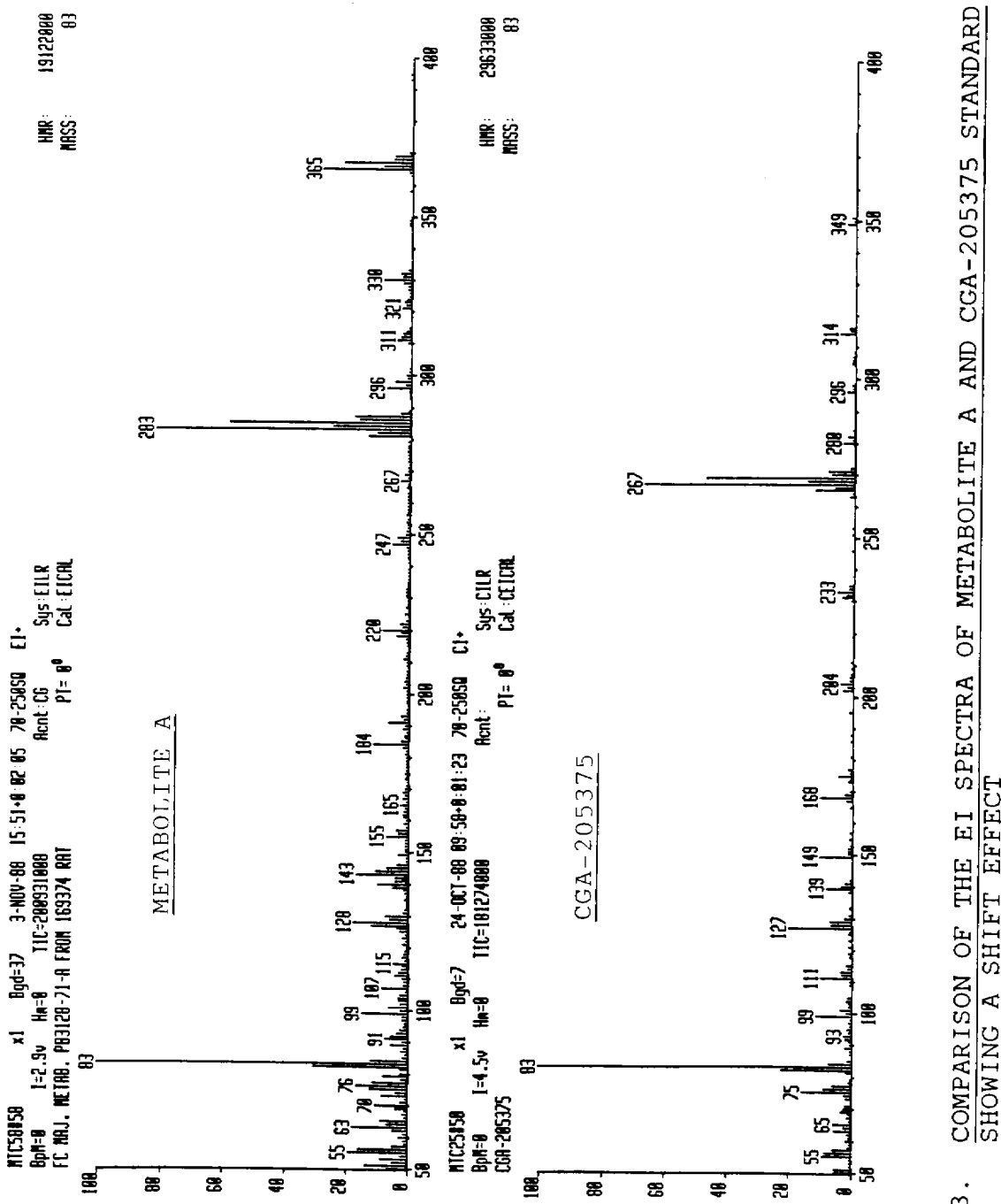


FIGURE 13.

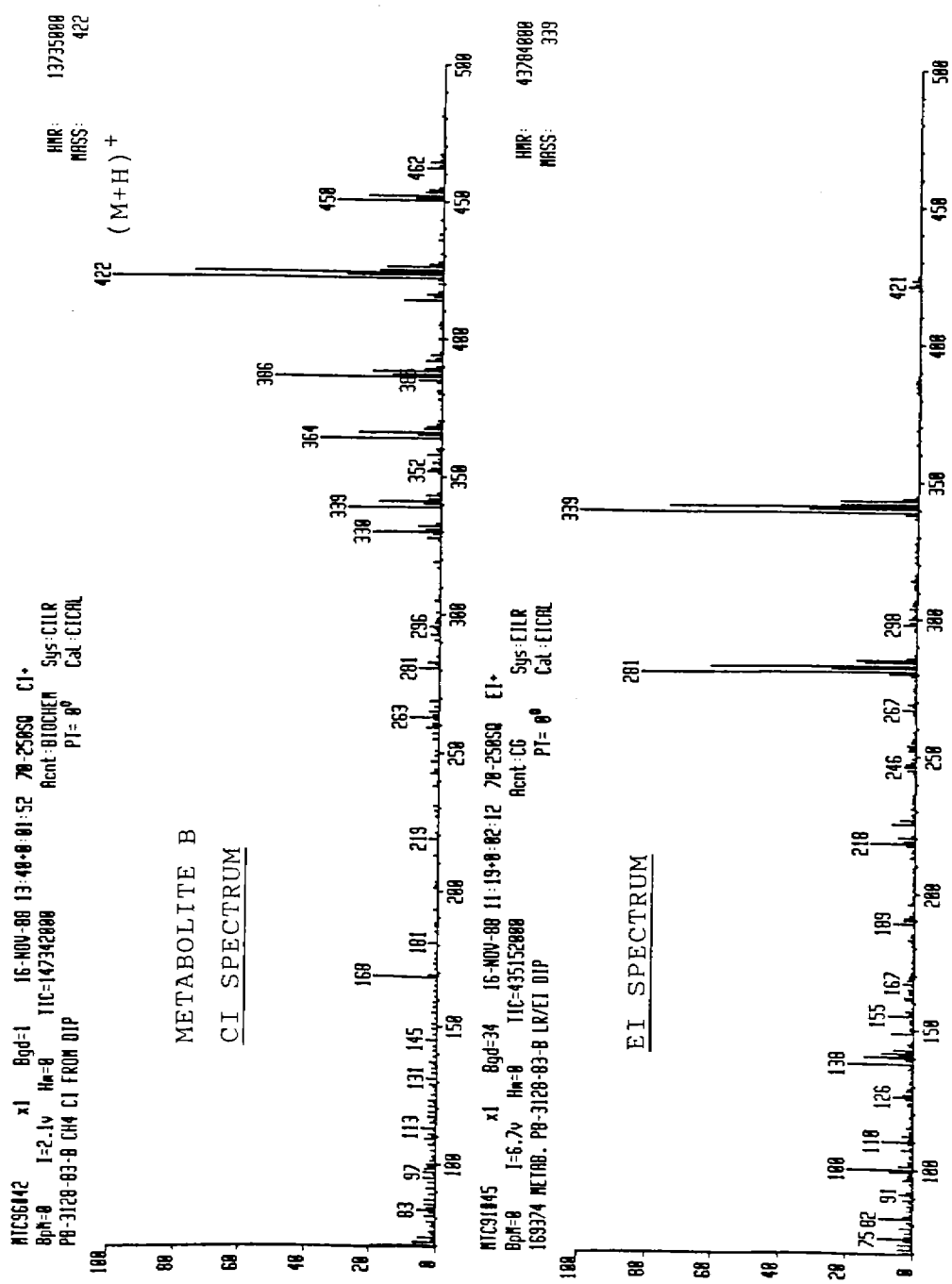
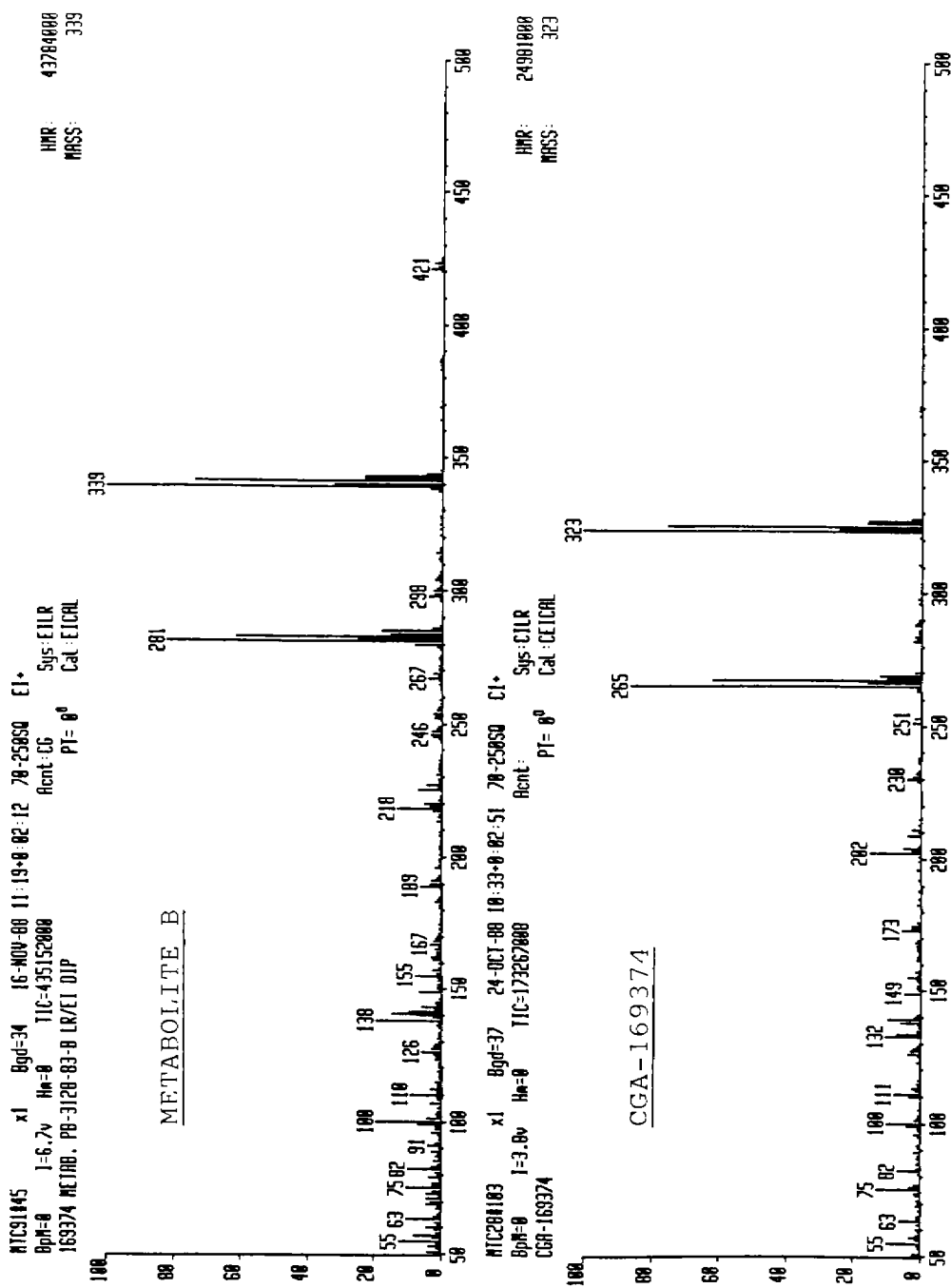


FIGURE 14. COMPARISON OF THE EI AND CI MASS SPECTRA OF METABOLITE B



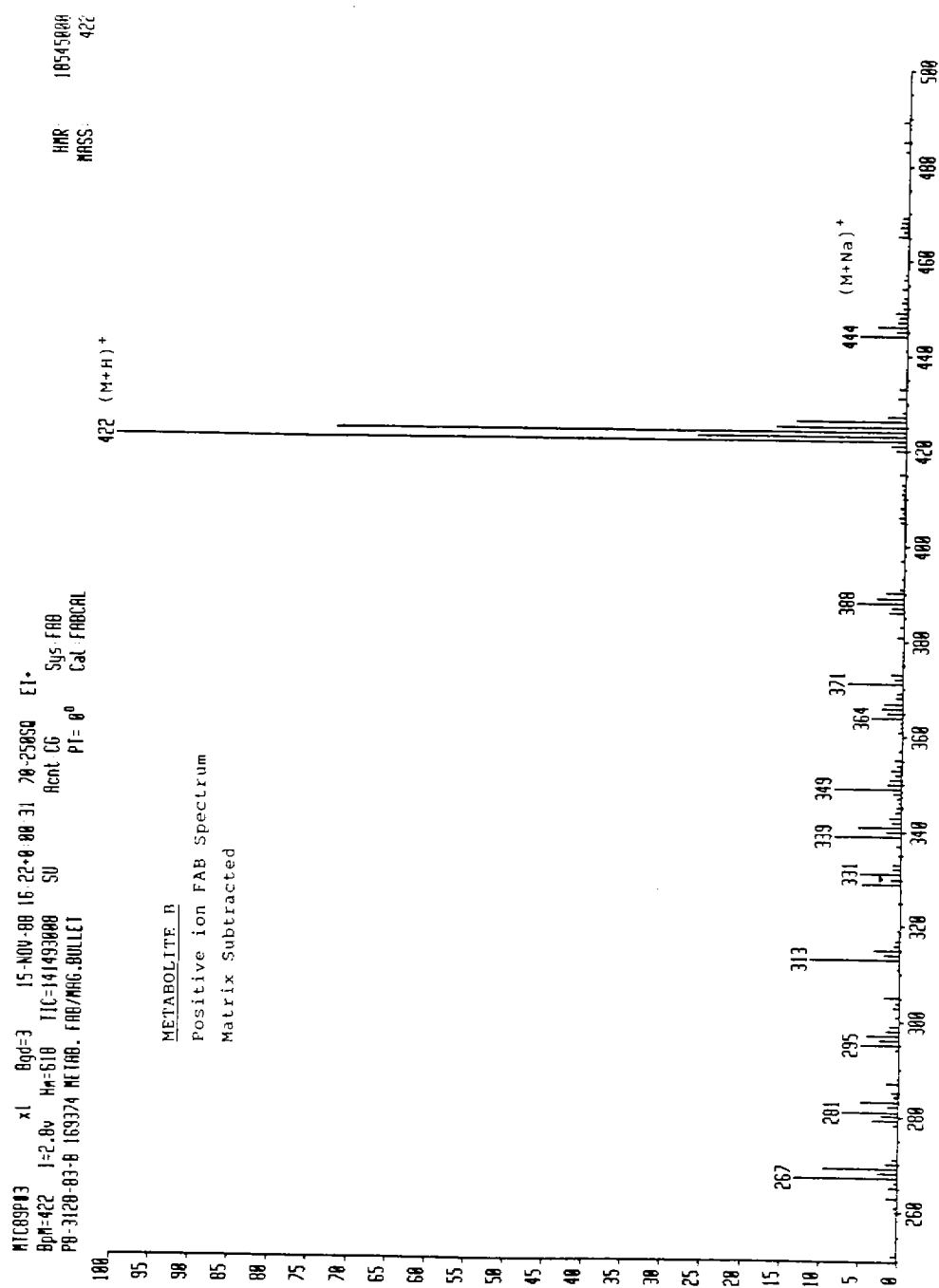


FIGURE 16. FAB SPECTRUM OF METABOLITE B

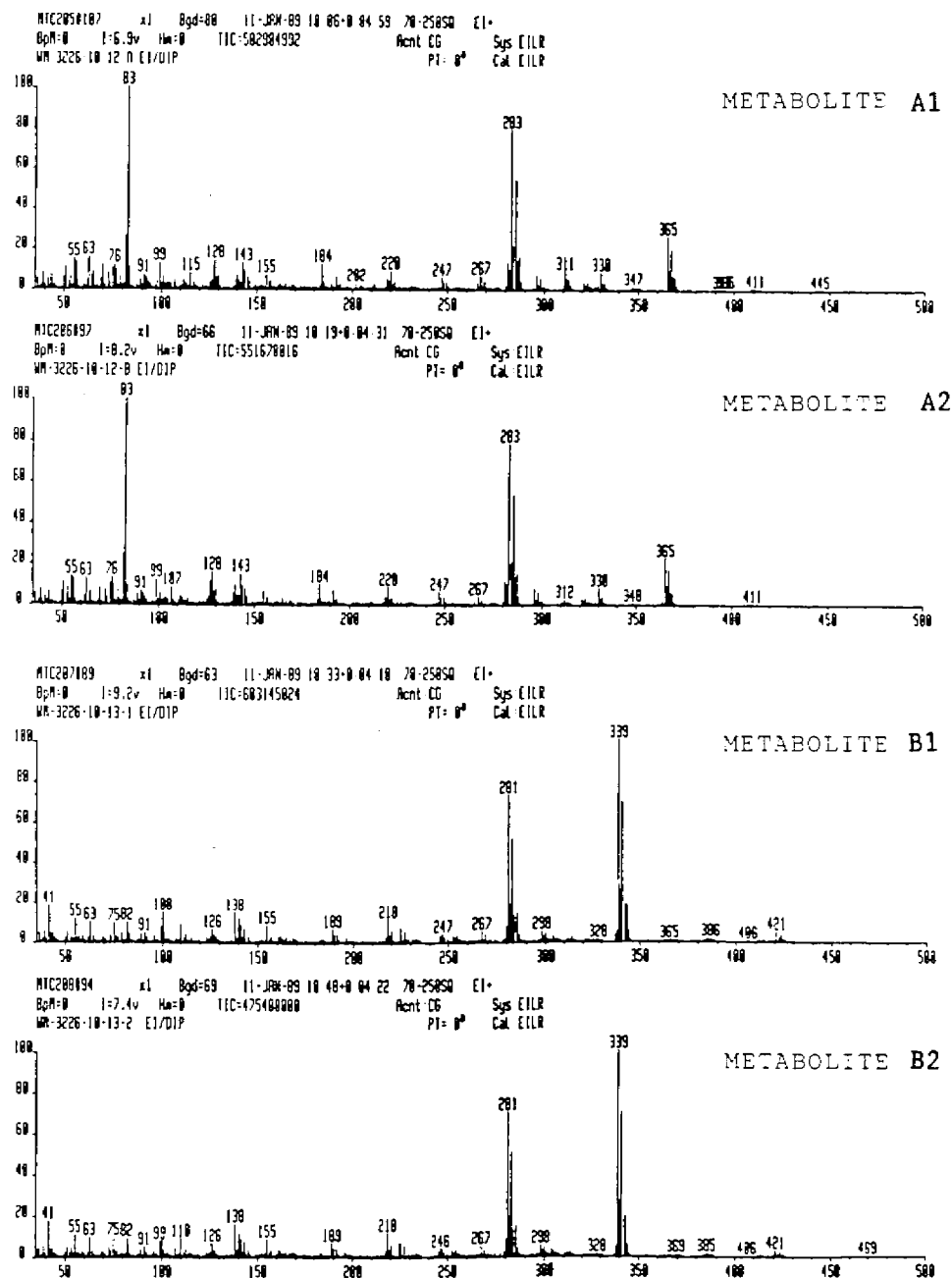
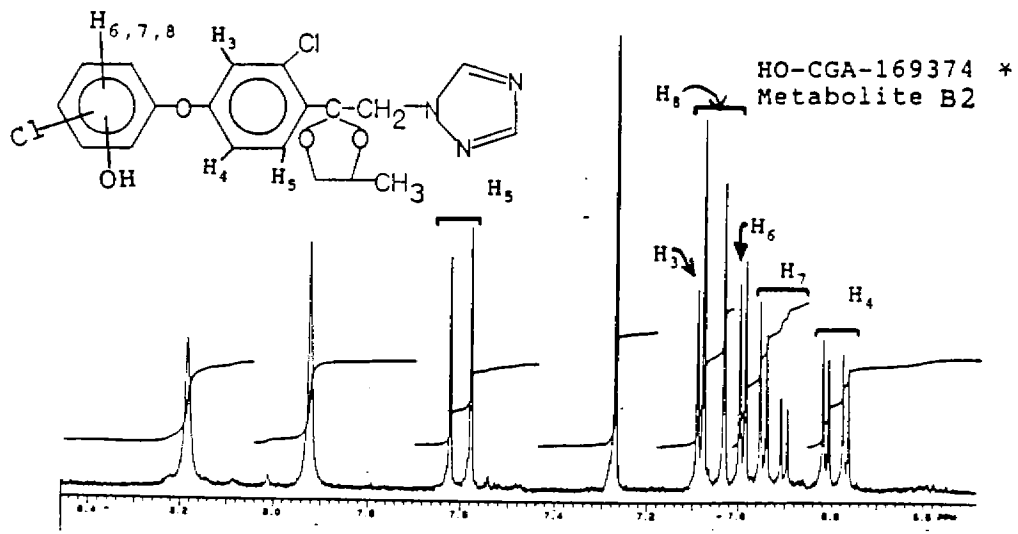
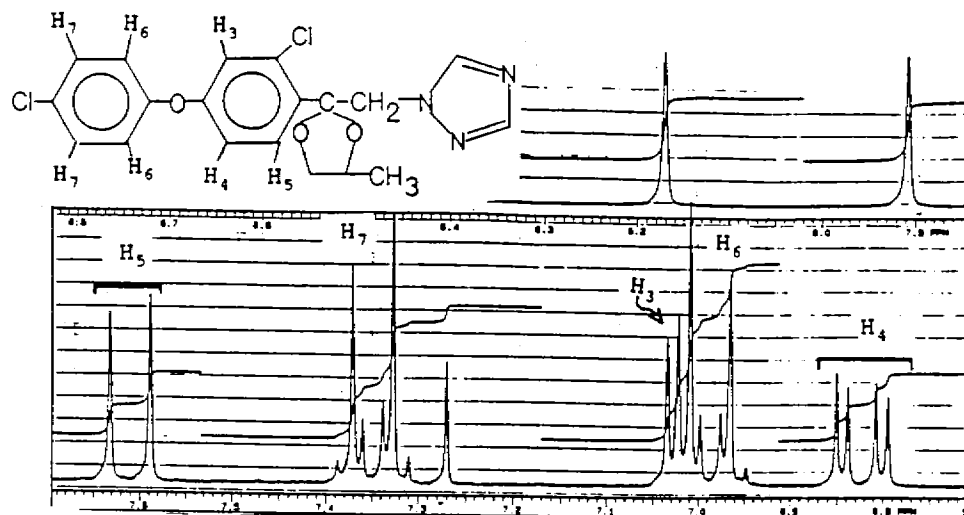


FIGURE 17. COMPARISON OF THE EI MASS SPECTRA OF THE PAIRS OF ISOMERS OF METABOLITES A AND B

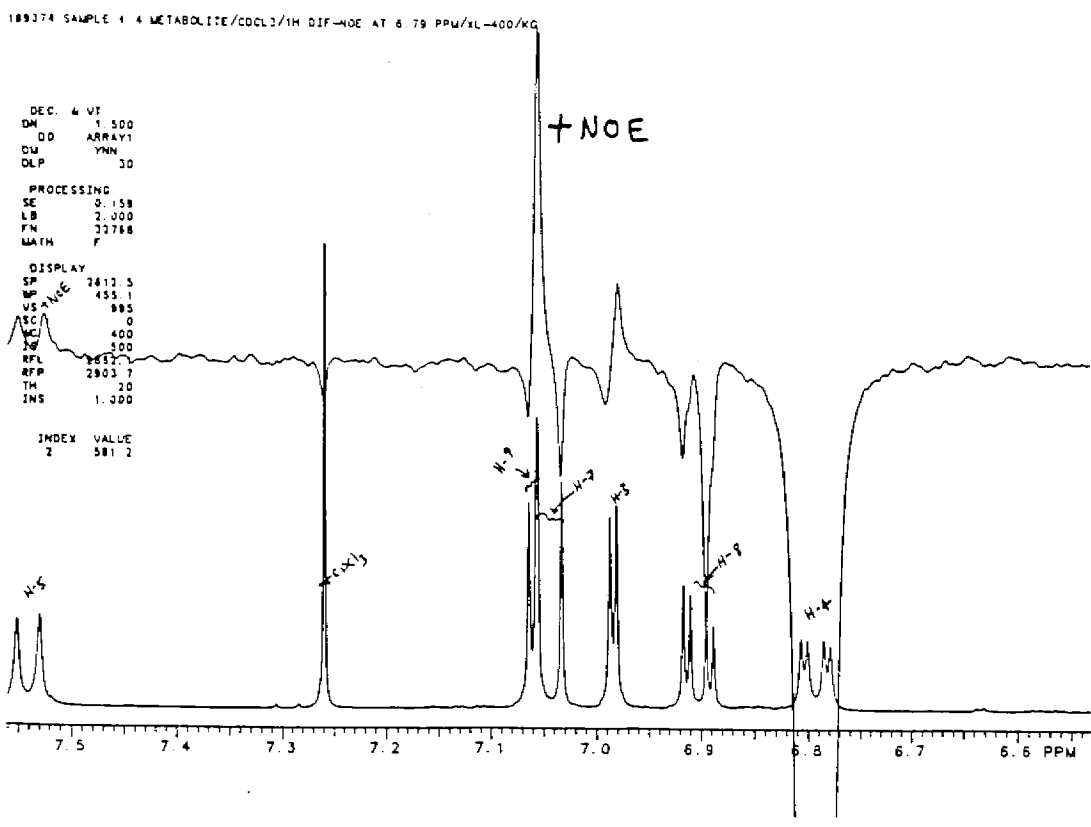
CGA-169374
one diastereomer



*Proton NMR demonstrates trisubstitution of outer ring only
(See Fig. 1, page 36 for exact structure of Metabolite B2.)

Outer ring coupling:
H₆ - meta doublet
H₇ - ortho, meta doublet of doublets
H₈ - ortho doublet

FIGURE 18. COMPARISON OF THE AROMATIC REGIONS OF THE
PROTON NMR SPECTRA OF METABOLITE B2 AND ONE
DIASTEREOMER OF CGA-169374



DIFFERENCE NOE EXPERIMENT - IRRADIATE H₄

ortho case-
NOE to meta doublet
(H₃) likely

meta case-
NOE to meta double
(H₃) improbable

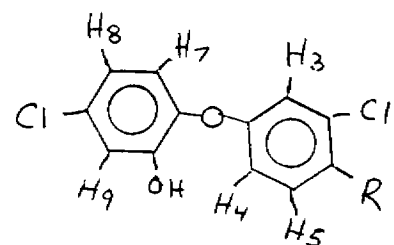
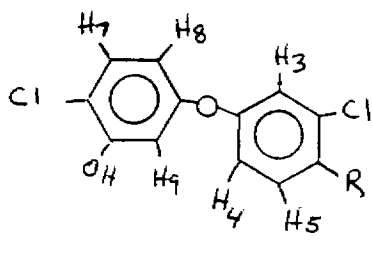


FIGURE 19. AROMATIC REGION OF A DIFFERENCE NOE PROTON NMR SPECTRUM OF METABOLITE B1 OBTAINED WITH IRRADIATION AT 6.79 PPM

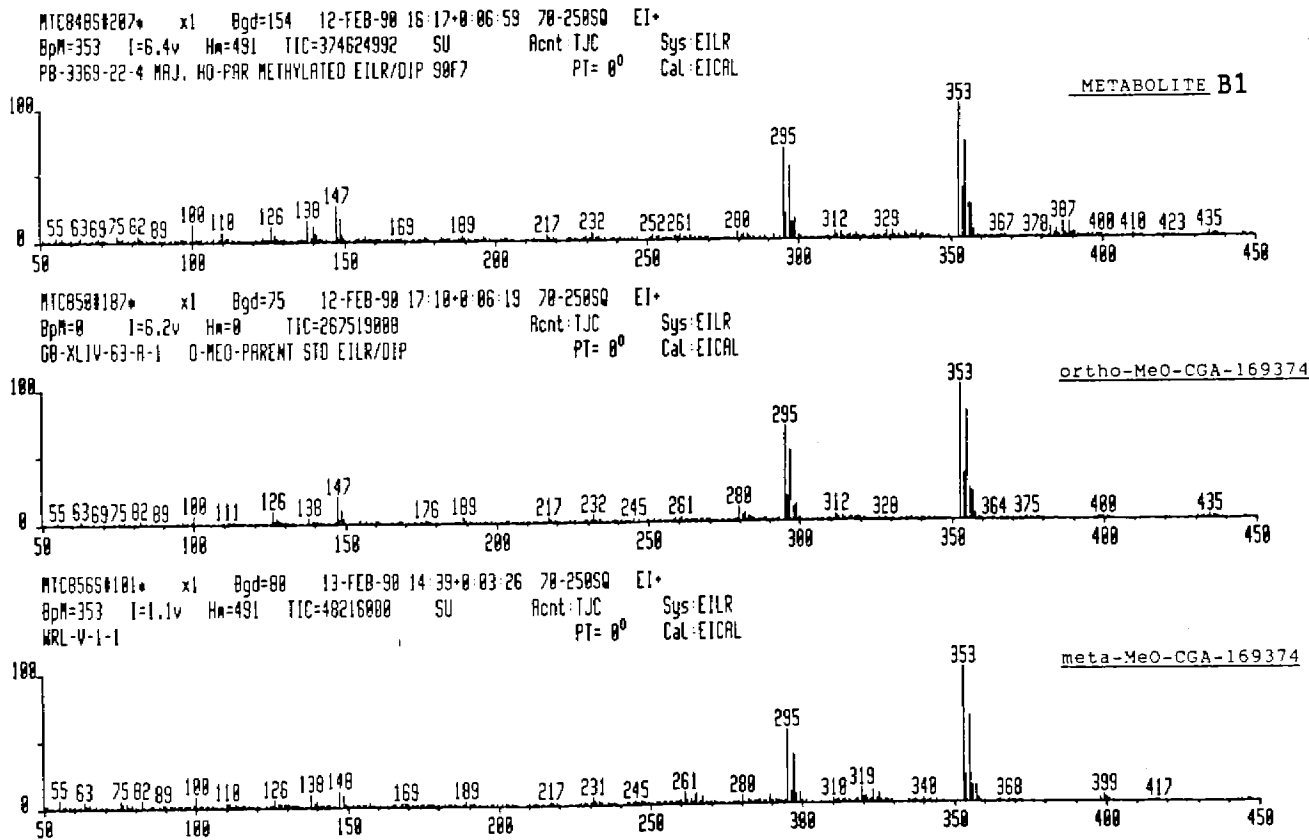


FIGURE 20. COMPARISON OF MASS SPECTRA OF METABOLITE B1
WITH ORTHO AND META METHOXY CGA-169374
STANDARDS

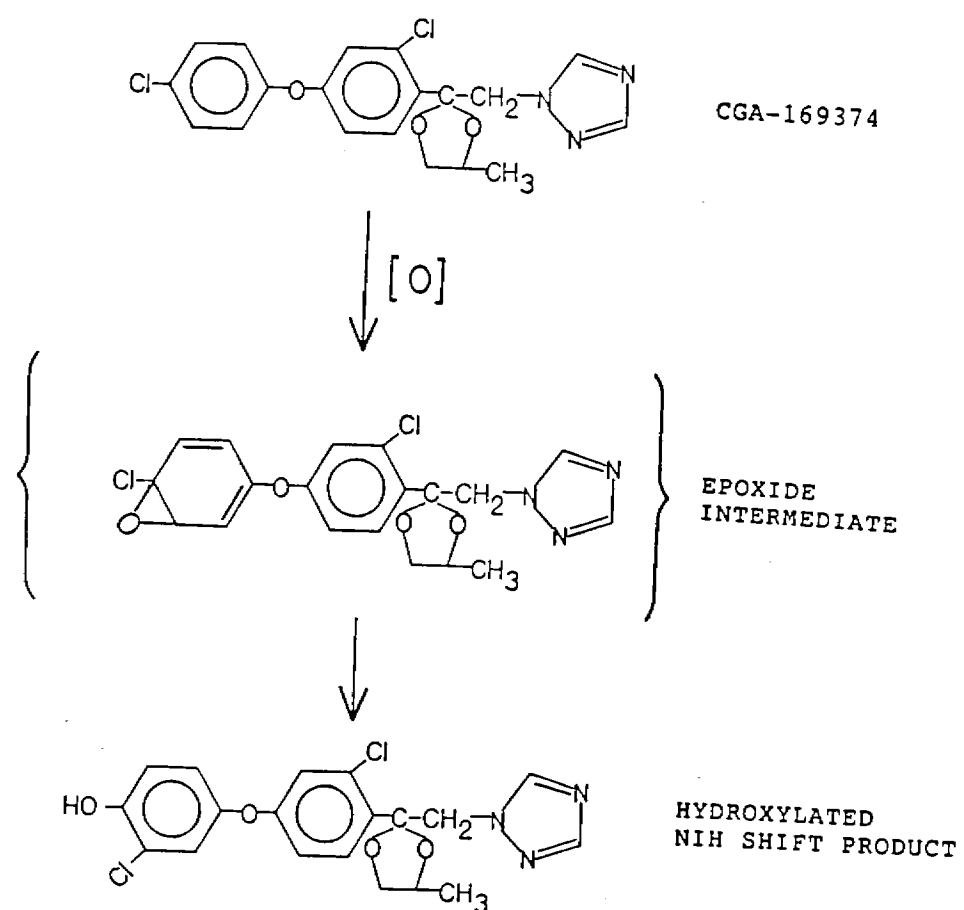


FIGURE 21. PLAUSIBLE MECHANISM FOR FORMATION OF
UNEXPECTED METABOLITE STRUCTURES BY THE NIH
SHIFT

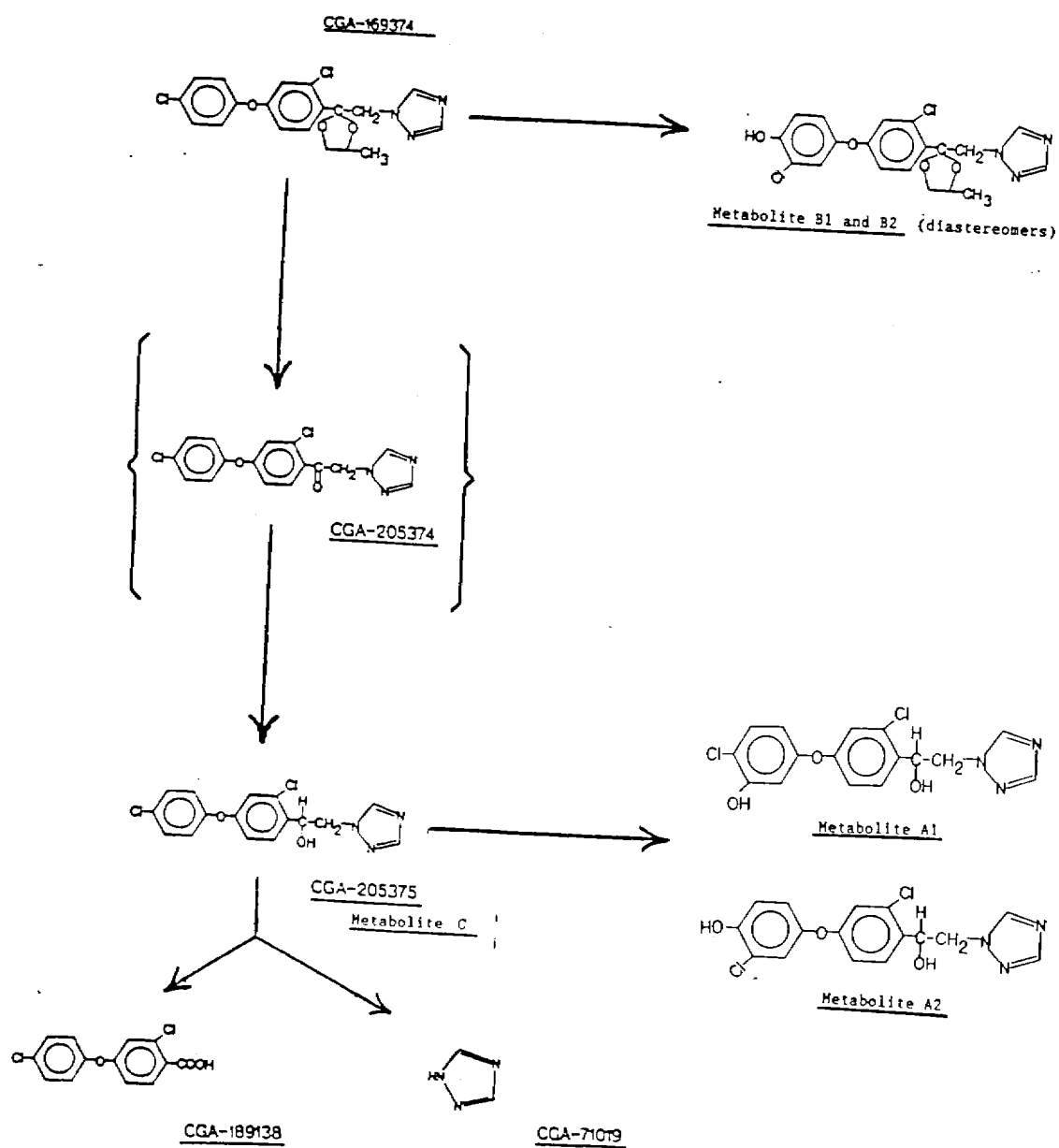


FIGURE 22. PROPOSED PATHWAY FOR THE METABOLISM OF CGA-169374 IN THE RAT

ACKNOWLEDGEMENT

The authors and study director are grateful for the outstanding technical support of W. Eberle, R. Rodebaugh, K. Gunderson, and the Chemical Synthesis group.

REFERENCES

1. McFarland, J. and Cassidy, J., "Metabolism of Triazole-¹⁴C and Phenyl-¹⁴C-CGA-169374 in the Rat - Distribution of Radioactivity," ABR-88043.
2. Craine, E. M., "Metabolism of Phenyl-¹⁴C-CGA-169374 in the Rat," WIL Research Laboratories, Inc., July 21, 1987, WIL-82013.
3. Craine, E. M., "Metabolism of Triazole-¹⁴C-CGA-169374 in the Rat," WIL Research Laboratories, Inc., July 21, 1987, WIL-82014.
4. Tanaka, F. S., Hoffer, B. L., Shimabukuro, R. H., Wien, R. G., and Walsh, W. C., J. Agric. Food Chem. 1990, 38, 559-565.
5. Maynard, M. and Brumback, D., "[¹⁴C]-CGA-169374 Phenyl and Triazole Label Distribution, Elimination, and Metabolism in Goats," ABR-89100.
6. Maynard, M. and Brumback, D., "[¹⁴C]-CGA-169374 Phenyl and Triazole Label Distribution, Elimination, and Metabolism in Hens," ABR-89101.
7. Hubbard, L., Harper, J., and Briley, A., "Uptake and Metabolism of ¹⁴C-CGA-169374 by Wheat Resulting from Foliar Spray Application in a Greenhouse Environment," ABR-90011.

Metabolism Department
Ciba Plant Protection
Ciba-Geigy Corporation
Greensboro, North Carolina

SUPPLEMENTAL REPORT ON THE METABOLISM OF
¹⁴C-PHENYL-CGA-169374 IN RATS - IDENTIFICATION OF
THE MAJOR URINARY METABOLITES

AMENDMENT 1

Report No.: ABR-90019 Project No.: 420988

Study Director:
Thomas M. Capps

Approved By:
William E. Swain, Jr.

Title: Sr. Group Leader
Animal Metabolism

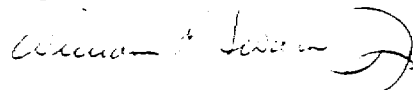
Title: Manager
Animal Metabolism

Signature:



Date: 3/4/93

Signature:



Date: 3/4/93

Submitted By: T. Capps
W. Anderson

Sponsor: Ciba-Geigy Corporation
Ciba Plant Protection
Metabolism Department
410 Swing Road
Post Office Box 18300
Greensboro, NC 27419

TABLE OF CONTENTS

	<u>PAGE NO.</u>
GLP COMPLIANCE STATEMENT	4
QUALITY ASSURANCE STATEMENT	5
GENERAL INFORMATION	6
SUMMARY	7
I. INTRODUCTION	7
II. MATERIALS	8
III. METHODS	8
IV. CIRCUMSTANCES AFFECTING THE STUDY	9
V. RESULTS AND DISCUSSION	9
VI. CONCLUSION	12
VII. LIST OF TABLES	
I. BALANCE DATA SUMMARY FROM ABR-88043	13
VIII. LIST OF FIGURES	
1. CHEMICAL NAMES AND STRUCTURES	14
2. HPLC COMPARISON OF HIGH DOSE, FEMALE, RAW URINE	17
3. FLOW DIAGRAM - HIGH DOSE FEMALE URINE	18
4. PREPARATIVE HPLC CHROMATOGRAM OF HIGH DOSE FEMALE URINE	19
5. TWO-DIMENSIONAL TLC OF PEAK 1 FROM PREPARATIVE HPLC	20
6. FAB/MS OF COMPONENT 1AS	21
7. FAB/MS DAUGHTER ION SPECTRA OF COMPONENT 1AS	22

TABLE OF CONTENTS
(continued)

	<u>PAGE</u> <u>NO.</u>
8. FAB/MS OF COMPONENT 1B2	23
9. TWO-DIMENSIONAL TLC OF REACTION PRODUCT OF 1BS and 1B2 WITH DIAZOMETHANE	24
10. TWO-DIMENSIONAL TLC OF PEAK 2 FROM PREPARATIVE HPLC	25
11. TWO-DIMENSIONAL TLC OF COMPONENT 2A AND UV STANDARD OF CGA-205375	26
12. FAB/MS OF COMPONENT 2A	27
13. FAB/MS DAUGHTER ION SPECTRA OF COMPONENT 2A	28
14. TWO-DIMENSIONAL TLC OF PEAK 3 FROM PREPARATIVE HPLC	29
15. FAB/MS OF COMPONENT 3B	30
16. FAB/MS DAUGHTER ION SPECTRA OF COMPONENT 3B	31
17. THERMOSPRAY/MS OF COMPONENT 3B	32
18. METABOLIC PATHWAY OF CGA-169374 IN RATS	33
IX. REFERENCES	34

GOOD LABORATORY PRACTICE COMPLIANCE STATEMENT

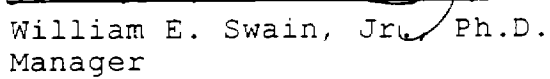
The additional work described in this report was conducted in accordance with the applicable EPA Good Laboratory Practice Standards (40 CFR Part 160).



Thomas M. Capps, Ph.D.
Study Director

3/4/93

Date



William E. Swain, Jr., Ph.D.
Manager

3/4/93

Date

Ciba-Geigy Corporation
Ciba Plant Protection
Quality Assurance Unit

QUALITY ASSURANCE STATEMENT

Final Report Amendment Title: SUPPLEMENTAL REPORT ON THE
METABOLISM OF ¹⁴C-PHENYL-CGA-169374 IN RATS -
IDENTIFICATION OF THE MAJOR URINARY METABOLITES

Study Director: T. M. Capps

Project Number: 420988

Protocol Number: 98-86 with Amendments

Pursuant to Good Laboratory Practice Regulations, this statement verifies that the aforementioned study was inspected and/or audited and the findings reported to Management and to the Study Director(s) by the Quality Assurance Unit on the dates listed below.

<u>Audit Type</u>	<u>Inspection/Audit Date</u>	<u>Reporting Date</u>
Final Report Audit	3/13-16/90 6/28, 7/3/90	3/19/90 7/3/90
In-Progress Inspection	1/15/93	2/9/93
Final Report Amendment 1	2/24-25/93	2/25/93

Prepared by:

Lisa Phelps
Lisa Phelps

Date: 2/25/93

GENERAL INFORMATION

Study Participants: W. Anderson, P. Barr, T. Capps,
T. Carlin, W. Eberle,
W. Meadows,

Test Material: Ciba Designation:
CGA-169374, 1-[2-[4-(4-chloro-
phenoxy)-2-chlorophenyl-(4-
methyl-1,3-dioxolan-2-yl)-
methyl]-1H-1,2,4-triazole

Testing Facilities: Biological Phase
WIL Research Laboratories,
Inc.
Ashland, OH 44805-9281

Analytical Phases I and II
Ciba-Geigy Corporation
Ciba Plant Protection
Metabolism Department
410 Swing Road
P. O. Box 18300
Greensboro, NC 27419

Study Initiation: December 4, 1986

Study Completion: March 4, 1993

Protocol Numbers: 98-86 (Phenyl) and Amendments¹
99-86 (Triazole) and
Amendments²

Archives: Protocols, raw biological data
and two biological reports
(WIL-82013 and WIL-82014) are
filed and archived at WIL
Research Laboratories, Inc.,
Ashland, OH.

A copy of the protocols, raw data
for Analytical Phase I and Phase
II, and these reports are filed
and archived in the Metabolism
and Residue Chemistry
Departments' archives,
L-Building, Ciba-Geigy
Corporation, Greensboro, NC. The
specimens related to these
reports are stored in the
Metabolism Residue Freezer,
Ciba-Geigy Corporation,
Greensboro, NC.

SUMMARY

As reported in the FIFRA rat study, ABR-90019³, 78-95% of the ¹⁴C-CGA-169374 residues were excreted in feces. The significant fecal metabolites were identified and resulted from hydroxylation of the outer phenyl ring followed by hydrolysis of the dioxane ring. The only significant urinary metabolite identified was free triazole, indicating bridge cleavage to be a minor metabolic pathway in rats.

In this report, the isolation and identification of urinary metabolites of rats treated with ¹⁴C-phenyl-CGA-169374 is reported. The urine sample investigated was from the high dose female group and accounted for 14.7% of the total dose.

The urinary metabolites were isolated by preparative HPLC and TLC followed by identification using mass spectrometry. Small quantities of free CGA-205375 (0.2%) and HO-CGA-205375 (1.7%) were present in the urine sample. The sulfate conjugates of these two metabolites accounted for 2.8% and 2.0% of the dose, respectively. Another minor product yielded mass spec data consistent with a hydroxy-acetic acid (ϕ -O- ϕ CHOH-COOH) and accounted for 1.8% of the total dose.

I. INTRODUCTION

CGA-169374, 1-[2-[4-(4-chlorophenoxy)-2-chlorophenyl-(4-methyl-1,3-dioxolan-2-yl)-methyl]]-1H-1,2,4-triazole, is a new fungicide being developed by Ciba-Geigy Corporation. The structures of this compound and its metabolites are shown in Figure 1.

An EPA review dated 7/23/92 of ABR-90019³ entitled, "Characterization and Identification of Major Triazole ¹⁴C and Phenyl-¹⁴C-CGA-169374 Metabolites in Rats," asked for additional identification of major peaks in urine of high dose female rats. This report contains the added information on urine metabolites of CGA-169374.

II. MATERIALS

Materials used in this study were the same as those described in ABR-90019³ with the following exceptions:

Day 1 urine samples from high dose ¹⁴C-phenyl female rats (#214, 216 and 218) were combined and filtered through an acrodisc nylon filter (Gelman) to remove particulates.

III. METHODS

Methods used in this study were the same as those described in ABR-90019³ with the following exceptions:

A. Radio-High Performance Liquid Chromatography: Radio-HPLC measurements were performed using unit 1:

UNIT 1: Perkin-Elmer Model 410 solvent delivery system
Perkin-Elmer LC 95 UV detector
at 281 nm
IN/US β -Ram Model 1A LC
Radiodetector Foxy Model 200
fraction collector

System-A1 was used for profiling the urine samples and system-A2 for preparative HPLC purifications; these systems are described in ABR-90019³.

B. Thin Layer Chromatography: The same systems as mentioned in ABR-90019³, but only the 20x20 cm precoated (250 micron) silica gel F-254 plates (Merck) were used. Radioactive zones were detected and quantitated using an AMBIS Radioanalytic Imaging System. The radioactive zones were located on the plate by using a light box and the 1:1 printout of the TLC plate from the AMBIS scanner. Visualization of standards and the areas to be scraped was done under ultraviolet light at 254 nm and recorded on Polaroid 100 Land film. Extraction of silica gel of the TLC plates was accomplished by scraping the ¹⁴C area of interest into methanol and stirring with

a magnetic stirring bar on a magnetic stir plate. The extract was filtered through F porosity scintered glass buchner funnels.

C. Calculations

Calculations were performed as described in ABR-90019³.

IV. CIRCUMSTANCES AFFECTING THE STUDY

No circumstances occurred that adversely affected the integrity or outcome of the study.

V. RESULTS AND DISCUSSION

A detailed analysis of the balance and identification in rats dosed with phenyl-¹⁴C-CGA-169374 and triazole-¹⁴C-CGA-169374 was presented in ABR-88043⁴ and ABR-90019.³

The objective of this supplemental work was to address EPA concerns for additional isolation and identification of the major urine metabolites of phenyl-¹⁴C-CGA-169374 from the FIFRA rat study.

Table I is reproduced from the earlier reports and shows the balance data for all dose levels and both labels. Total urinary elimination ranged from 8 to 22%. The total percent of dose urinary elimination from ¹⁴C-phenyl and ¹⁴C-triazole labels are similar for all dose groups.

The urine samples from high dose female rats treated with phenyl-¹⁴C-CGA-169374 were selected for this identification work, since the profile had previously been reported (ABR-90019)³.

Isolation and Identification of Major Urinary Metabolites

Day 1 urine from the high dose female rats was utilized for isolation and identification in this work since Day 2 and Day 3 urine had been virtually depleted in the earlier study. The Day 1 urine sample was profiled by HPLC

using system A1. A comparison of the urine samples (Figure 2) shows the metabolic pattern to be qualitatively the same with some quantitative differences.

A flow diagram (Figure 3) is included which illustrates the approach and the results obtained.

The Day 1 urine sample was subjected to preparative HPLC using system A2 to yield peaks 1,2 and 3 (Figure 4) which accounted for 6%, 3.9% and 2.0% of the total dose, respectively.

Peak 1

Peak 1 (6% of dose) was subsequently separated by preparative 2D-TLC (Figure 5) into components 1AS, 1A2, 1BS and 1B2. Component 1AS was analyzed by negative ion FAB/MS (Figure 6) and showed a molecular ion cluster at m/z 444 and m/z 446 indicative of the presence of two chlorine atoms in the molecule. A negative daughter ion spectrum (Figure 7) of m/z 444 shows a strong fragment at m/z 364. This loss of 80 mass units is equivalent to loss of SO_3 . The mass spec data taken in consideration with the very polar nature of the metabolite supports the structure of 1AS to be the sulfate conjugate of HO-CGA-205375. 1AS accounts for 2% of the total dose.

Component 1A2 was analyzed by FAB/MS, but the data was inconclusive. 1A2 was subjected again to 2D-TLC system yielding components 1A2-1 (0.5%) and 1A2-2 (1.0%). Based on the chromatographic similarity to 1AS by TLC and HPLC, and extreme polarity, components of 1A2 are proposed to be sulfate conjugates isomeric with 1AS. Component 1A2 accounted for 1.6% of the dose with no single component exceeding 1.1% of the total dose.

Components 1BS and 1B2 (Figure 5) were also analyzed by negative ion FAB/MS. The MS data from 1BS was inconclusive, but a parent ion spectrum of m/z 110 was obtained for 1B2 (Figure 8) which showed a molecular ion cluster at m/z 364 and m/z 366. This data

suggests the presence of HO-CGA-205375. Components 1BS and 1B2 were combined and methylated with diazomethane. The reaction product was subjected to 2D-TLC along with isomeric standards of $\text{CH}_3\text{O}-\text{CGA}-205375$ (Figure 9). By quantitation, 82.9% of the reaction product cochromatographed with the methylated standards CGA-277162 and CGA-277163. Based on the preceding results, 1BS and 1B2 are isomers of HO-CGA-205375 and account for 1.7% of the total dose.

Peak 2

Peak 2 (3.9% of the dose) was separated by preparative 2D-TLC (Figure 10) into components 2A and 2B which comprised 3.1% and 0.3% of the dose, respectively. Component 2A was again purified by prep 2D-TLC which yielded 2A and a minor component (Figure 11). The minor component was shown by FAB/MS and cochromatography with a synthetic standard to be CGA-205375 and accounted for 0.2% of the dose. Component 2A was analyzed by FAB/MS (Figure 12) and showed a molecular ion cluster at m/z 428 and m/z 430, a characteristic 2 chlorine pattern. A negative daughter ion spectrum of m/z 428 (Figure 13) showed an abundant ion at m/z 97, which was assigned as HSO_4^- . Based on these data, component 2A is the sulfate conjugate of CGA-205375 and accounts for 2.8% for the total dose (Figure 3). This structure is also supported by NMR data. Peak 2B (0.3%) was not investigated further.

Peak 3

Peak 3 (2.0% of the dose) was separated by preparative 2D-TLC (Figure 14) into components 3A and 3B which comprised 0.2% and 1.8% of the dose, respectively. Component 3A was not investigated further. Component 3B was analyzed by FAB/MS (Figure 15) and showed a weak molecular ion cluster at m/z 311 and m/z 313, a characteristic 2 chlorine pattern. Also present in the spectra is an ion cluster at m/z 333 and m/z 335 and another ion cluster at m/z 425 and m/z 427. The true molecular ion cluster ($\text{M}-\text{H}$)⁻ is at m/z 311, 313; the cluster at m/z 347, 349 is assigned

as $(M^- + Na^+ - H)^{-}$ and the cluster at m/z 425, 427 is assigned as $(M^- - Na^+ - H)^{-}$:glycerol adduct. A negative daughter ion spectrum of m/z 425 shows a loss of 92 mass units which is equivalent to glycerol. A negative daughter ion spectrum of m/z 311 showed fragments at m/z 267 and 127 which are characteristic of the dichloro diphenyl ether ring system (Figure 16). Further support for the molecular ion cluster at m/z 311 and m/z 313 was derived through negative thermospray MS (Figure 17). The above information is consistent with the structure of 3B being the hydroxyacetic acid ($\phi-O-\phi-CHOH-COOH$) metabolite which accounts for 1.8% of the total dose.

VI. CONCLUSION

The major metabolites of CGA-169374 in rats have now been identified. No single unknown urine metabolite accounts for more than 1.1% of the dose. With one exception, all of the urine metabolites that have been identified are metabolites that have been previously identified or are conjugates of these known metabolites. The hydroxyacetic acid urinary metabolite (1.8% of dose), along with the acid metabolite (CGA-189138) found in liver, are the only examples of bridge cleaved phenyl specific metabolites in rats. It appears likely, as a result of the limited bridge cleavage that does occur, the triazole and the hydroxyacetic acid metabolites are excreted in urine because of their polar nature while the free (phenyl) acid is absorbed by the tissues due to its lipophilic character. The metabolic pathway of CGA-169374 in rats is shown in Figure 18.

TABLE I. BALANCE DATA SUMMARY FROM ABR-88043

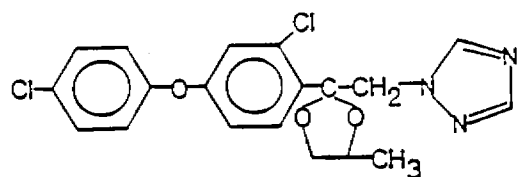
PHENYL-¹⁴C-CGA-169374

% Dose	SD	LOW DOSE		HIGH DOSE		HIGH DOSE		PRECOND.	
		MALE	FEMALE	MALE	FEMALE	MALE	FEMALE	MALE	FEMALE
Tissues	.60	.06	.36	.11	0.98	.14	.60	.17	1.04
Cage Wash	.22	.10	.12	.12	.24	.08	.99	.47	.24
Urine	12.93	1.36	17.19	3.66	8.48	2.81	14.70	3.95	19.25
Feces	86.72	6.05	81.38	6.79	94.61	2.91	85.36	4.85	78.95
Total	100.47		99.05		104.31		101.65		99.48

TRIAZOLE-¹⁴C-CGA-169374

% Dose	SD	LOW DOSE		HIGH DOSE		HIGH DOSE		PRECOND.	
		MALE	FEMALE	MALE	FEMALE	MALE	FEMALE	MALE	FEMALE
Tissues	.01	.02	.00	.00	.02	.01	.01	.00	.00
Cage Wash	0.20	0.19	.00	.00	.21	.07	.53	.48	.08
Urine	21.86	3.37	19.68	5.42	10.17	1.60	11.50	3.19	20.42
Feces	85.68	6.14	81.46	3.83	88.51	3.89	87.83	2.57	78.33
Total	107.75		101.14		99.45		99.87		98.83

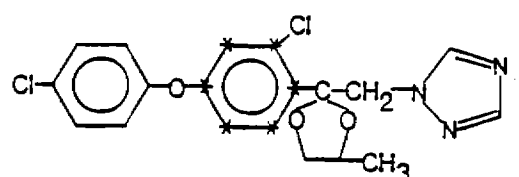
ABR-90019
Page 13 of 34



CGA-169374

1-[[2-[2-Chloro-4-(4-chlorophenoxy)phenyl]-4-methyl-1,3-dioxolan-2-yl]methyl]-1H-1,2,4-triazole

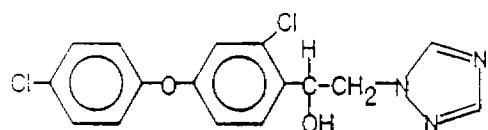
MW = 406.27



P-¹⁴C-CGA-169374

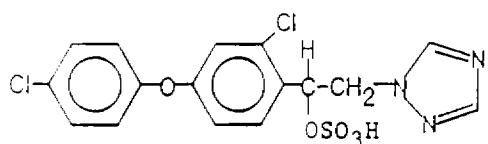
1-[[2-[2-Chloro-4-(4-chlorophenoxy)-[U-ring-¹⁴C]-phenyl]-4-methyl-1,3-dioxolan-2-yl]methyl]-1H-1,2,4-triazole

MW = 406.27



CGA-205375

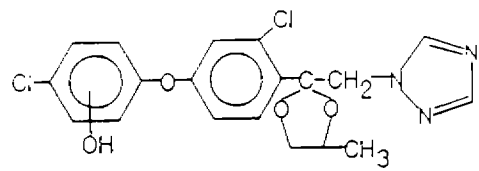
MW = 350



CGA-205375

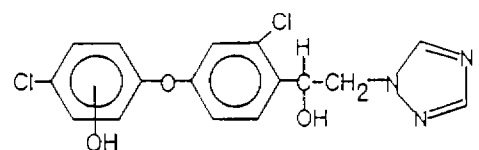
Sulfate Conjugate

FIGURE 1. CHEMICAL NAMES AND STRUCTURES



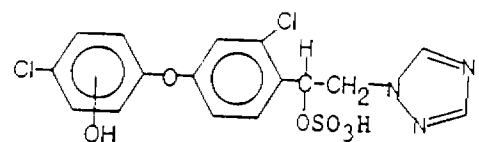
Hydroxy-CGA-169374

MW = 422



Hydroxy-CGA-205375

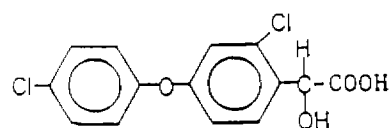
MW = 366



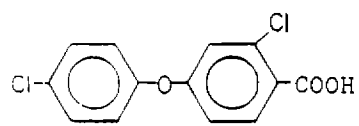
Hydroxy-CGA-205375

Sulfate Conjugate

FIGURE 1. CHEMICAL NAMES AND STRUCTURES
(Continued)

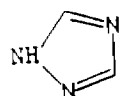


Hydroxy Acetic Acid



CGA-189138

MW = 283



CGA-71019

MW = 69

FIGURE 1. CHEMICAL NAMES AND STRUCTURES
(Continued)

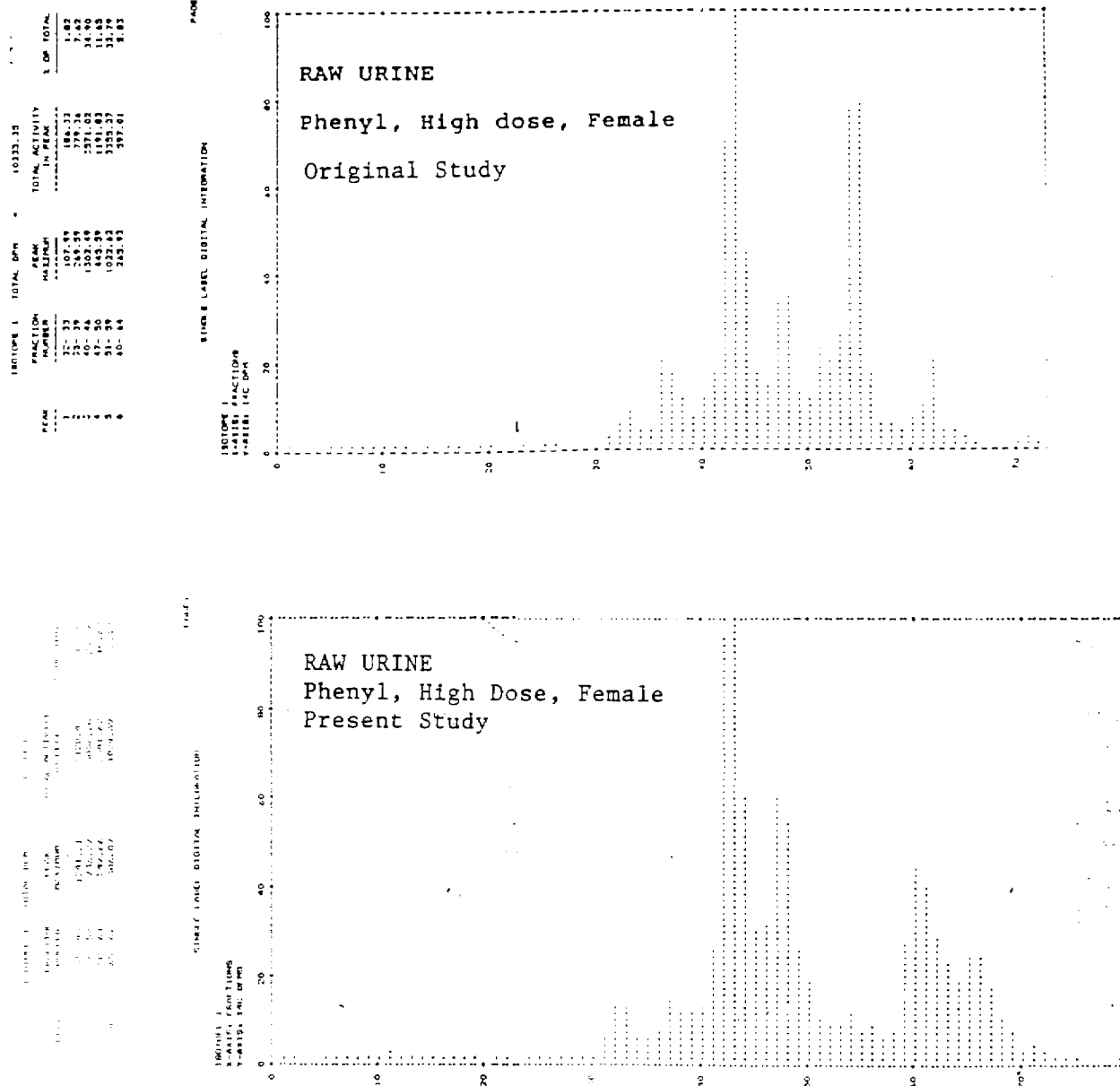


FIGURE 2. HPLC COMPARISON OF HIGH DOSE, FEMALE, RAW URINE

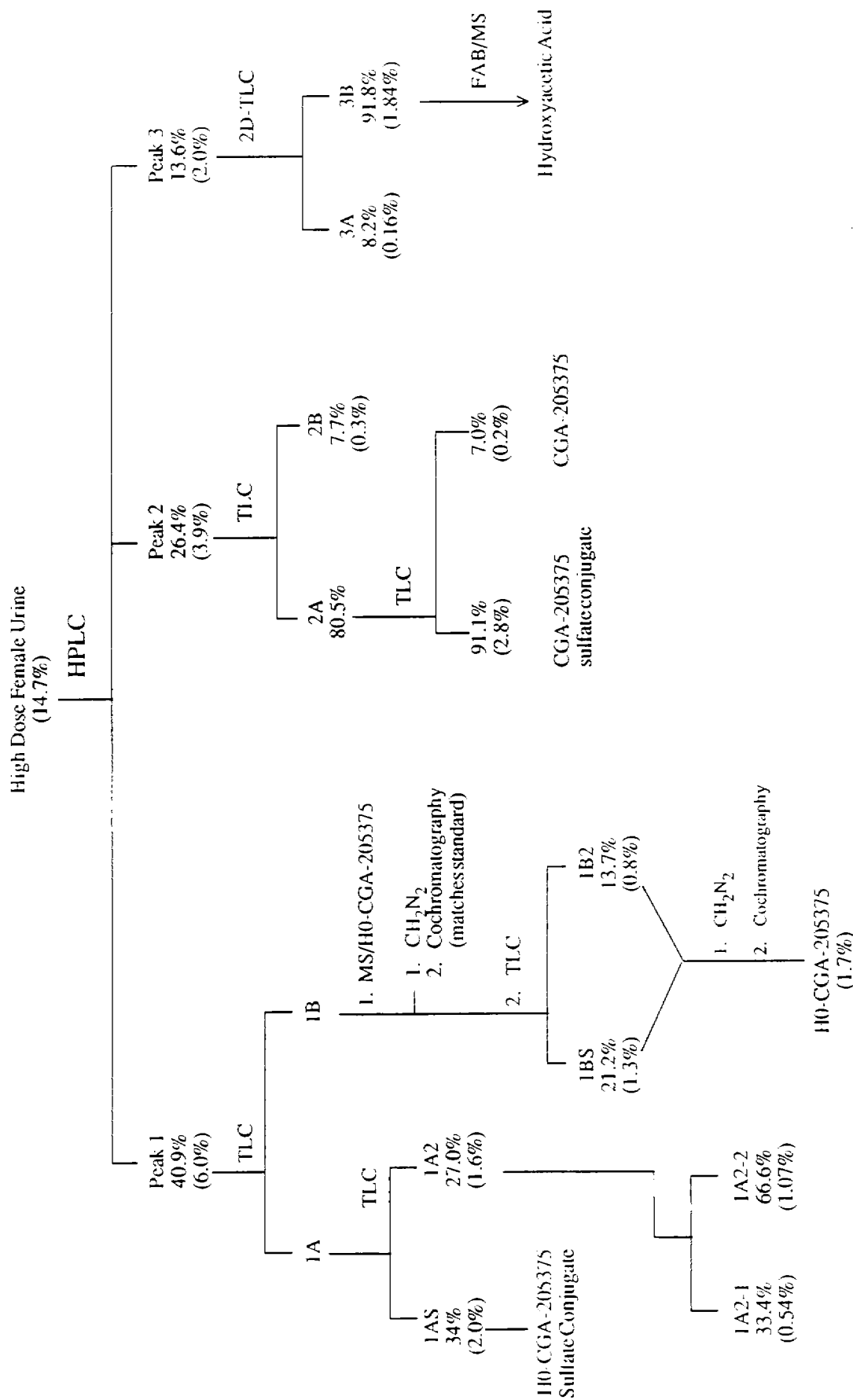


FIGURE 3. FLOW DIAGRAM - HIGH DOSE FEMALE URINE

() = represents percentage of total dose.

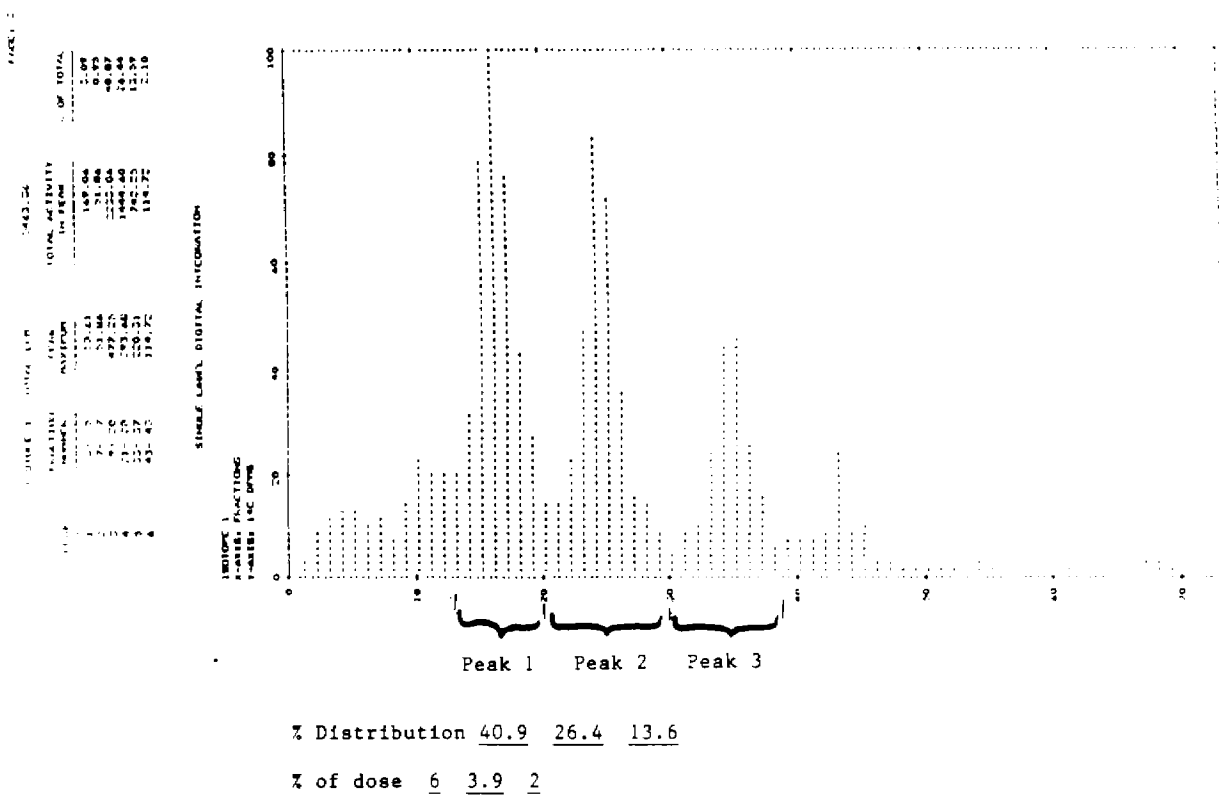


FIGURE 4. PREPARATIVE HPLC CHROMATOGRAM OF HIGH DOSE FEMALE URINE

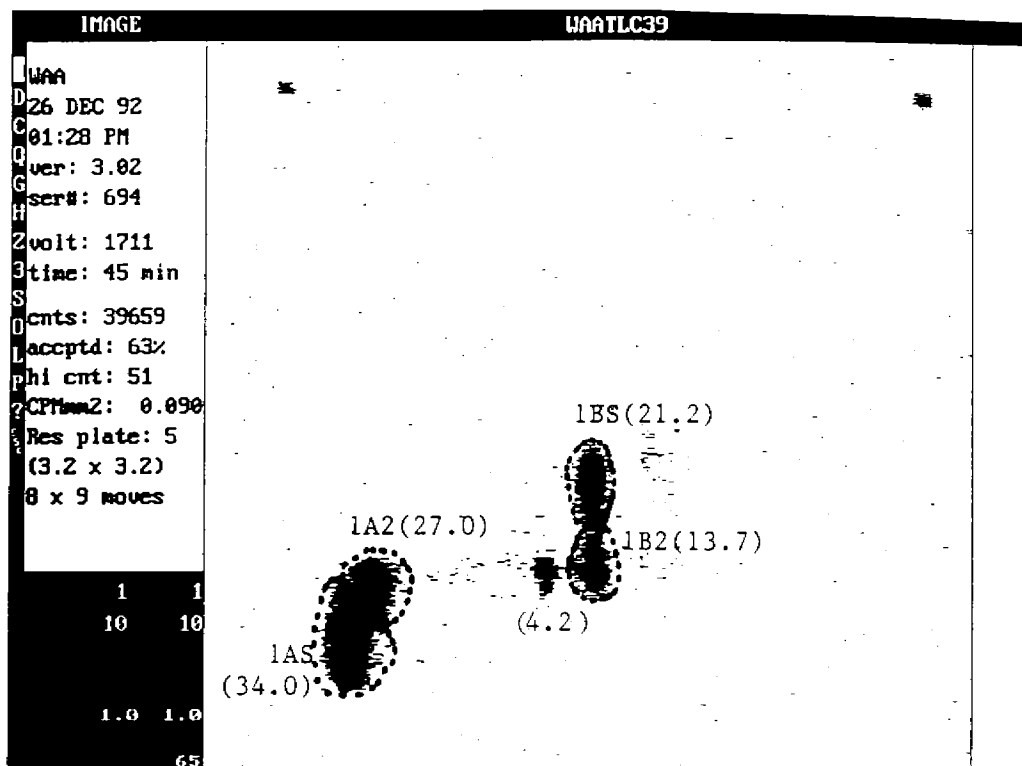


FIGURE 5. TWO-DIMENSIONAL TLC OF PEAK 1 FROM
PREPARATIVE HPLC

SPEC: tcf1589 31-DEC-92 DERIVED SPECTRUM 9
Samp: 1AS Start : 11:04:38 31
Comm: - FAB glycerol matrix Xe gas kV 0.5 mamp
Mode: FAB -Q3MS LMR UP LR Study : MS92D40 Pr 98-86
Oper: Carlin Client: W. Anderson Inlet : DIP
Base: 255.0 Inten : 1156987 Masses: 100 > 600
Norm: 255.0 RIC : 54627156 #peaks: 473
Peak: 1000.00 mmu Defect: 0 @ 1, 300 @ 1000
Data: +/-3>20

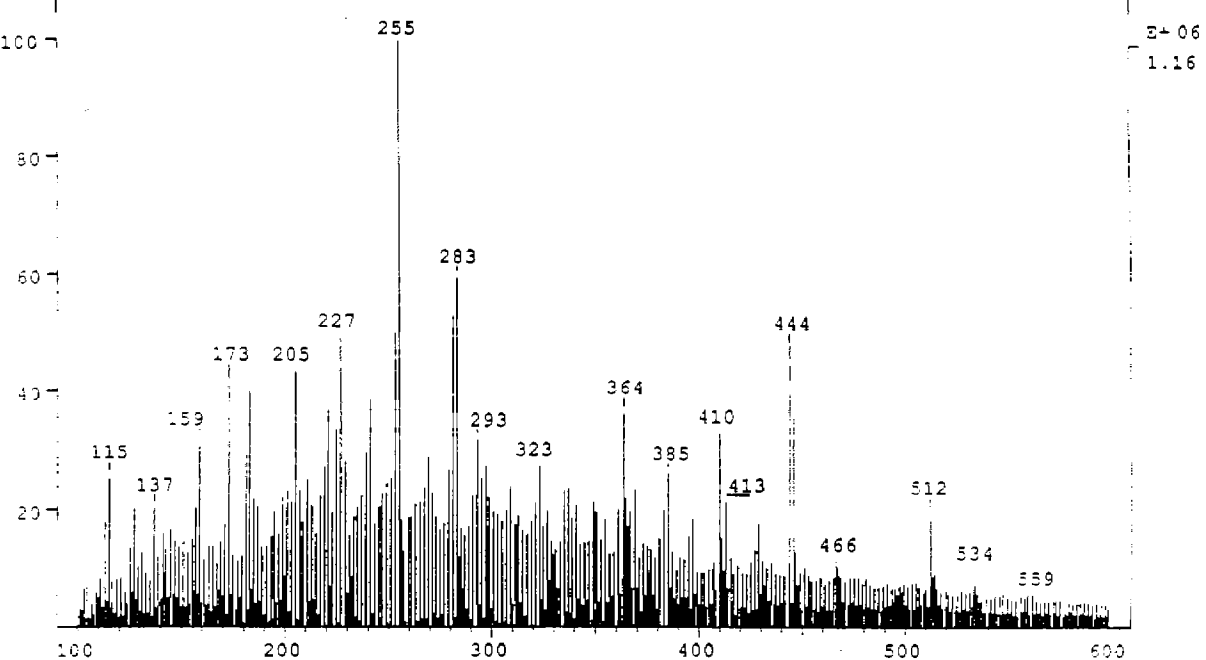


FIGURE 6. FAB/MS OF COMPONENT 1AS

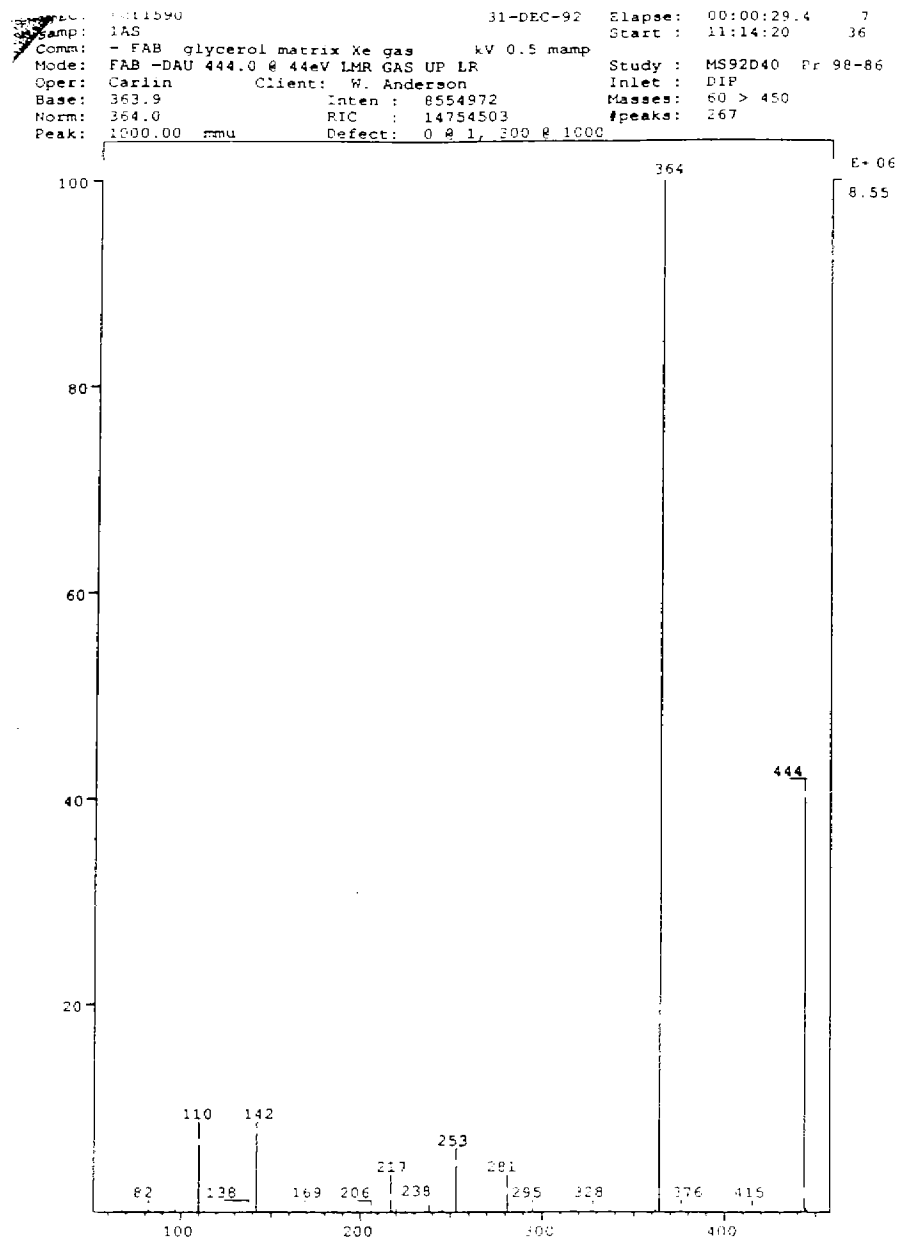


FIGURE 7. FAB/MS DAUGHTER ION SPECTRA OF
COMPONENT 1AS

SPEC: tcf1595 31-DEC-92 DERIVED SPECTRUM 9
Samp: 1B2 Start : 13:09:34 87
Comm: - FAB glycerol matrix Xe gas kV 0.5 mamp
Mode: FAB -PAR 110.0 @ 35eV LMR GAS UP LR Study : MS92D43 Pr 98-86
Oper: Carlin Client: W. Anderson Inlet : DIP
Base: 111.0 Inten : 2899 Masses: 70 > 600
Norm: 111.0 RIC : 17967 #peaks: 297
Peak: 1000.00 mamu Defect: 0 @ 1, 300 @ 1000
Data: +/-36>82

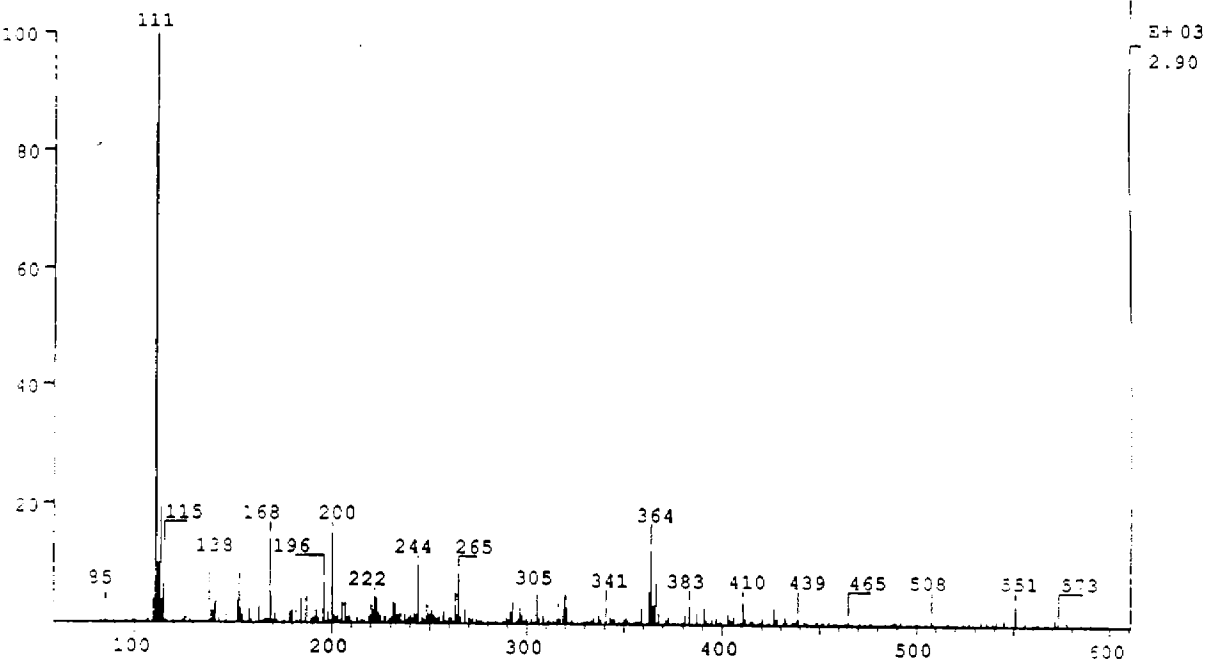
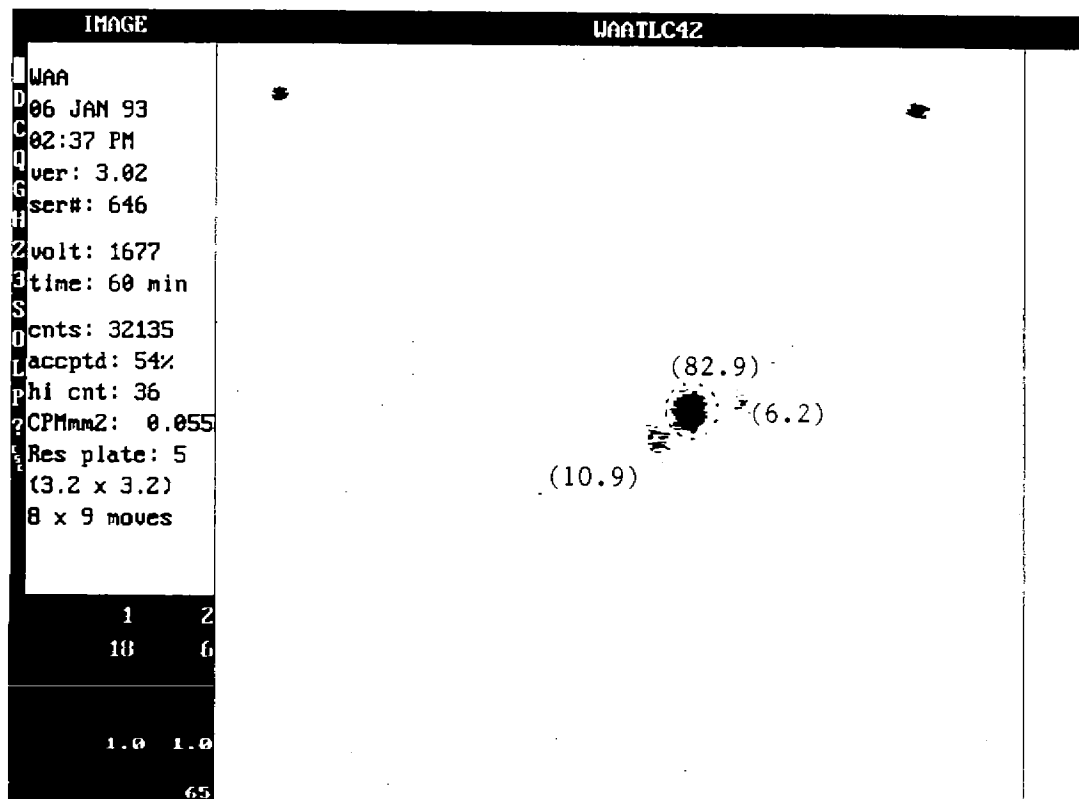


FIGURE 8. FAB/MS OF COMPONENT 1B2

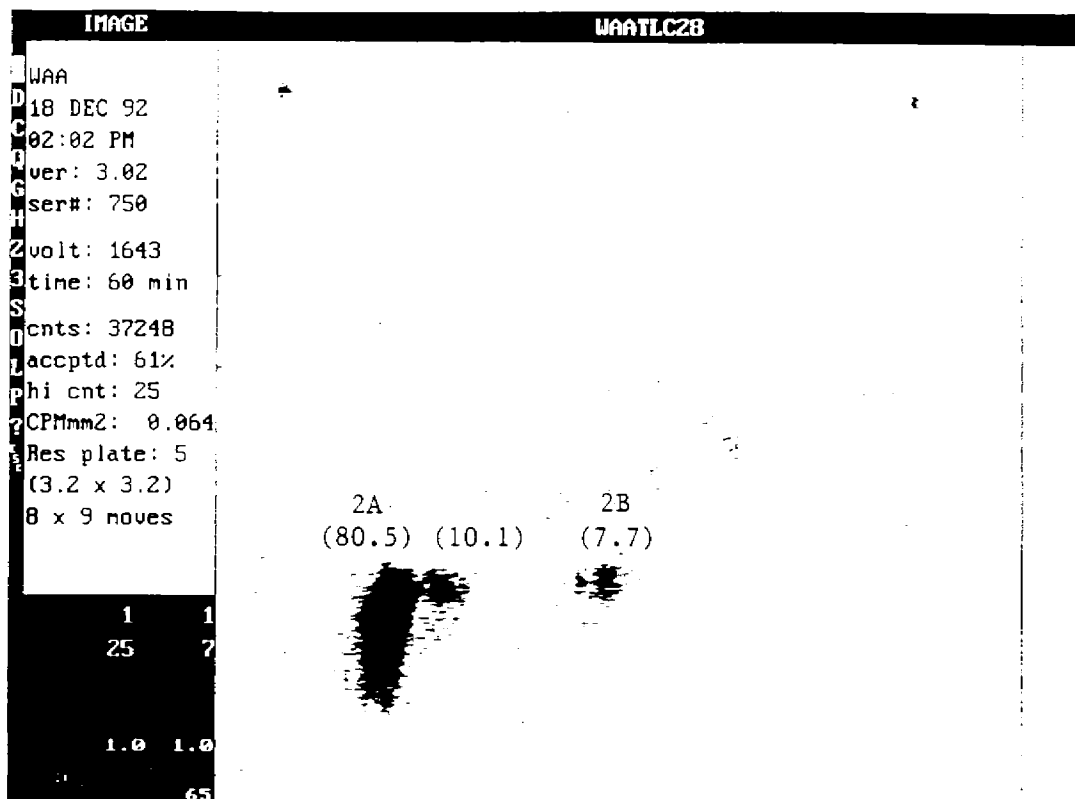


● = ^{14}C Zones

○ = UV Spot of Standards CGA-277162 and CGA-277163

() = TLC % Distribution

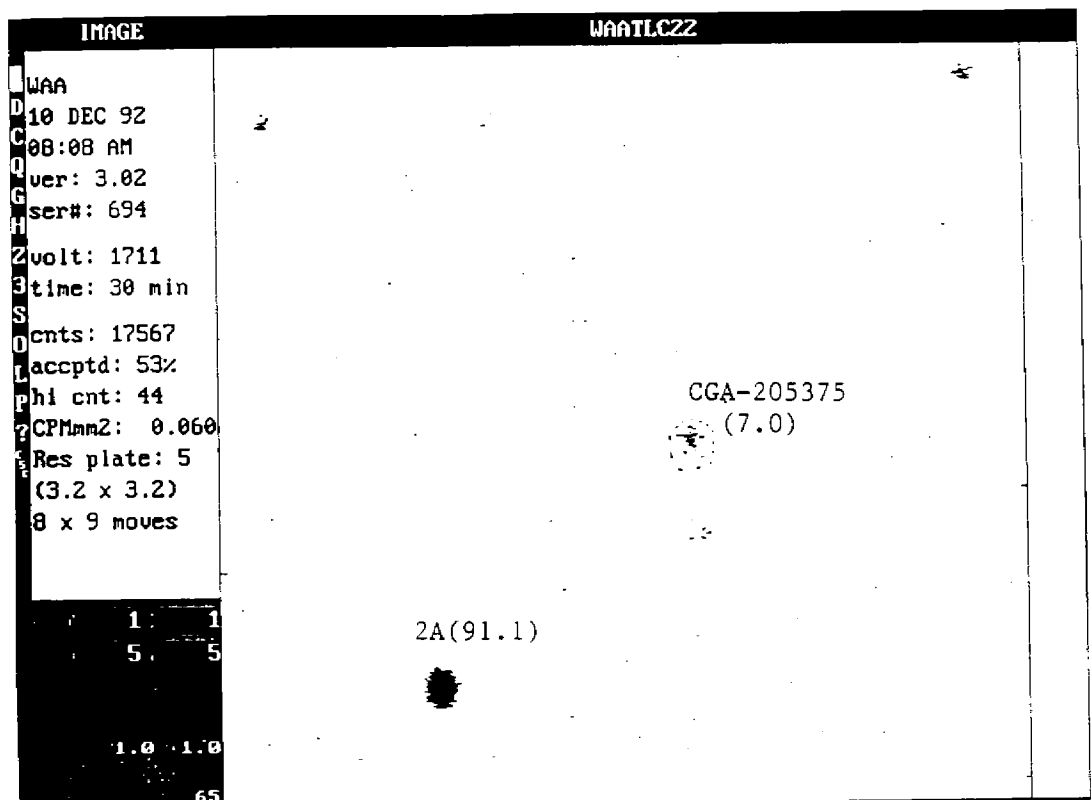
FIGURE 9. TWO-DIMENSIONAL TLC OF REACTION PRODUCT OF 1BS AND 1B2 WITH DIAZOMETHANE



● = ^{14}C Zones

() = TLC % Distribution

FIGURE 10. TWO-DIMENSIONAL TLC OF PEAK 2 FROM PREPARATIVE HPLC



● = ^{14}C Zones

○ = UV Zones

() = TLC % Distribution

FIGURE 11. TWO-DIMENSIONAL TLC OF COMPONENT 2A AND
UV STANDARD OF CGA-205375

SPEC: tcf1569 23-DEC-92 DERIVED S 9
 Samp: 2A 12/22/92 Start : 1 40
 Comm: +/- FAB glycerol matrix Xe gas xV 0.5 mamp
 Mode: FAB -Q1MS IMR UP LR Study : 3 Pr 98-86
 Oper: Carlin Client: W. Anderson Inlet :
 Base: 183.0 Inten : 1392565 Masses: 600
 Norm: 183.0 RIC : 25895629 *peaks:
 Peak: 1000.00 amu Defect: 0 @ 1, 300 & 1000
 Data: +/-16>29 ()

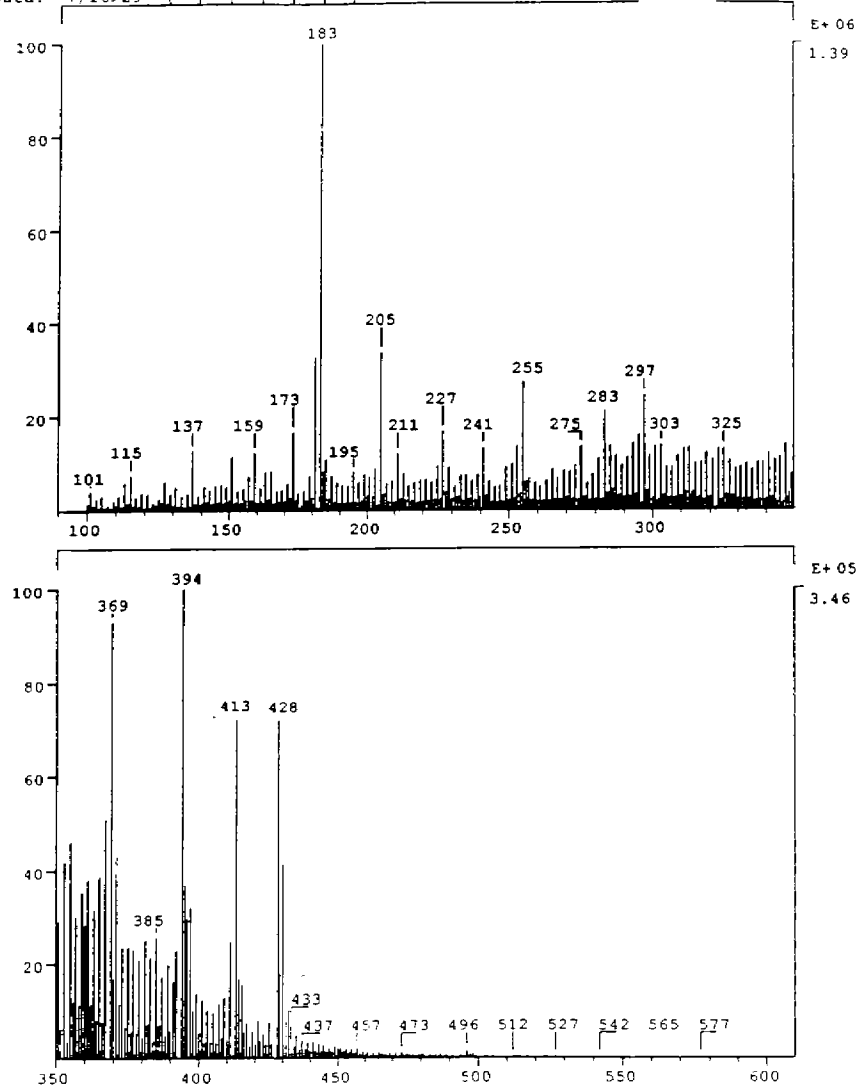


FIGURE 12. FAB/MS OF COMPONENT 2A

SPEC: tcf1572
Samp: 2A 12/22/92
+/- FAB glycerol matrix Xe gas kV 0.5 mamp
DAU 428.0 @ 35eV LMR GAS UP LR
n Client: W. Anderson
Inten : 70824 Study : MS92D33 Pr 98-86
Norm: 97.0 RIC : 122816 Inlet : DIP
Peak: 1000.00 mamu Defect: 0 @ 1, 300 @ 1000 Masses: 60 > 450
Data: +/16>22 #peaks: 102

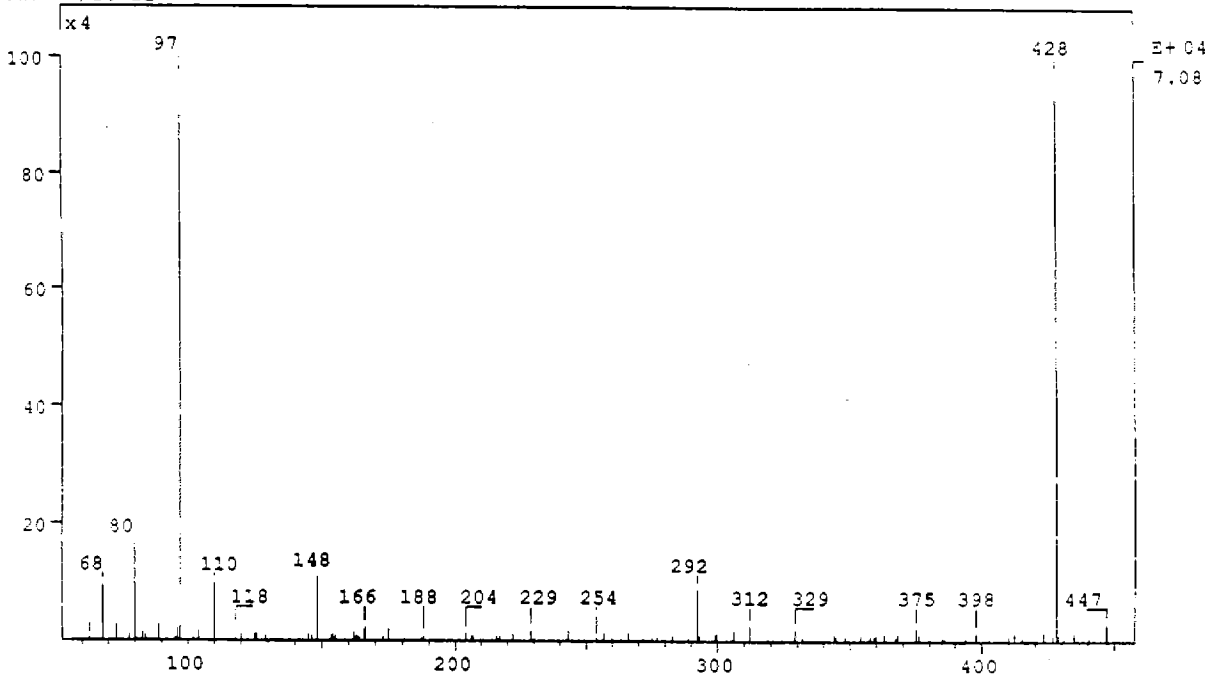
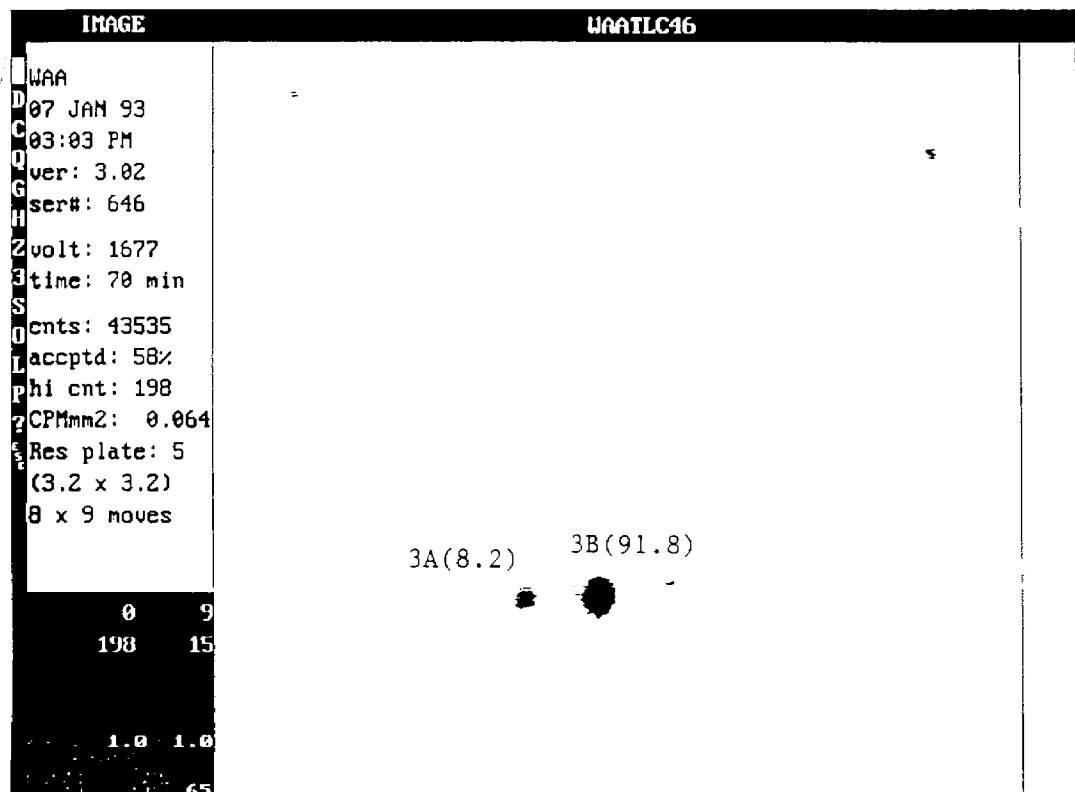


FIGURE 13. FAB/MS DAUGHTER ION SPECTRA OF COMPONENT 2A



● = ^{14}C Zones

() = TLC % Distribution

FIGURE 14. TWO-DIMENSIONAL TLC OF PEAK 3 FROM
PREPARATIVE HPLC

SPEC: ms93055 08-JAN-93 Elapse: 00:01:28.6 55
Samp: 3B Start: 14:12:43 58
Comm: +/- FAB glycerol matrix Xe gas kV 0.5 mamp
Mode: FAB-Q3MS LYR UP LR Study: MS93J26 Pr 98-86
Oper: Eberle Client: W. Anderson Inlet: DIP
Base: 183.0 Inten: 16200880 Masses: 40 > 550
Norm: 255.0 RIC: 584045628 #peaks: 459
Peak: 1000.00 mmu Defect: 0 @ 1, 300 @ 1000
Accu: 37 > 52

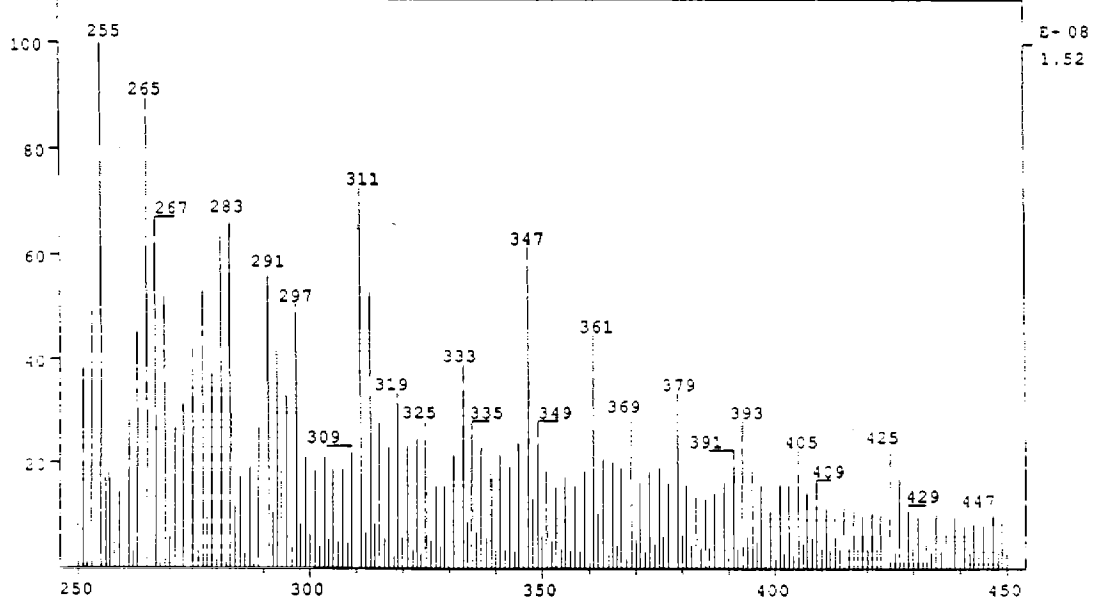


FIGURE 15. FAB/MS OF COMPONENT 3B

SPEC: ms93072 19-JAN-93 Elapse: 00:01:03.7 61
Samp: 3B Start : 11:04:42 117
Comm: +/- FAB glycerol matrix Xe gas KV 0.5 mamp
Mode: FAB -DAU 311.1 @ 29eV LMR GAS UP LR Study : MS93J26 Pr 98-86
Oper: Eberle Client: W. Anderson Inlet : DIP
Base: 311.0 Inten : 1618458 Masses: 20 > 350
Norm: 311.0 RIC : 3527679 #peaks: 333
Peak: 1000.00 mru Defect: 0 @ 1, 300 @ 1000

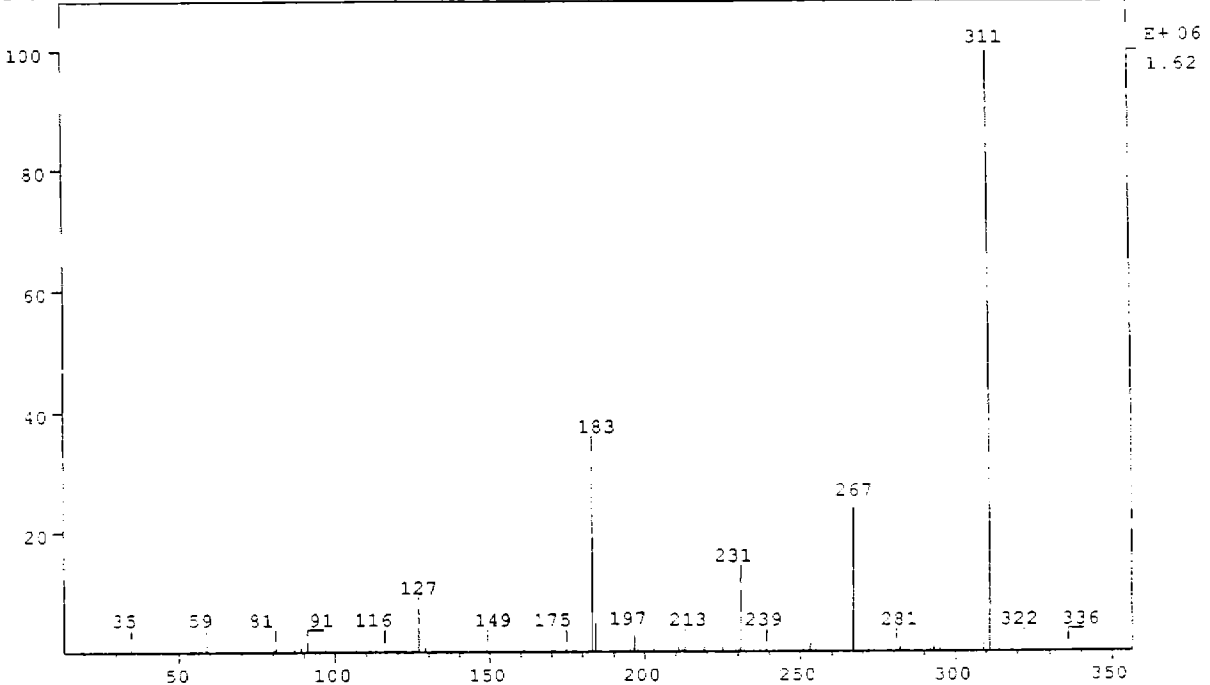


FIGURE 16. FAB/MS DAUGHTER ION SPECTRA OF COMPONENT 3B

SPEC: ms93060 11-JAN-93 DERIVED SPECTRUM 9
Samp: 3B Start : 13:53:29 28
Comm: +/- TSP Direct 1 ml/min 50:50 0.1N NH4OAc/MeOH
Mode: TSP -Q1MS LMR UP LR Study : MS93J26 Pr 98-86
Oper: Eberle Client: W. Anderson Inlet :
Base: 105.0 Inten : 285144 Masses: 100 > 600
Norm: 283.0 RIC : 408344 #peaks: 317
Peak: 1000.00 mru Defect: 0 @ 1, 300 @ 1000
Data: +/-22 - /3

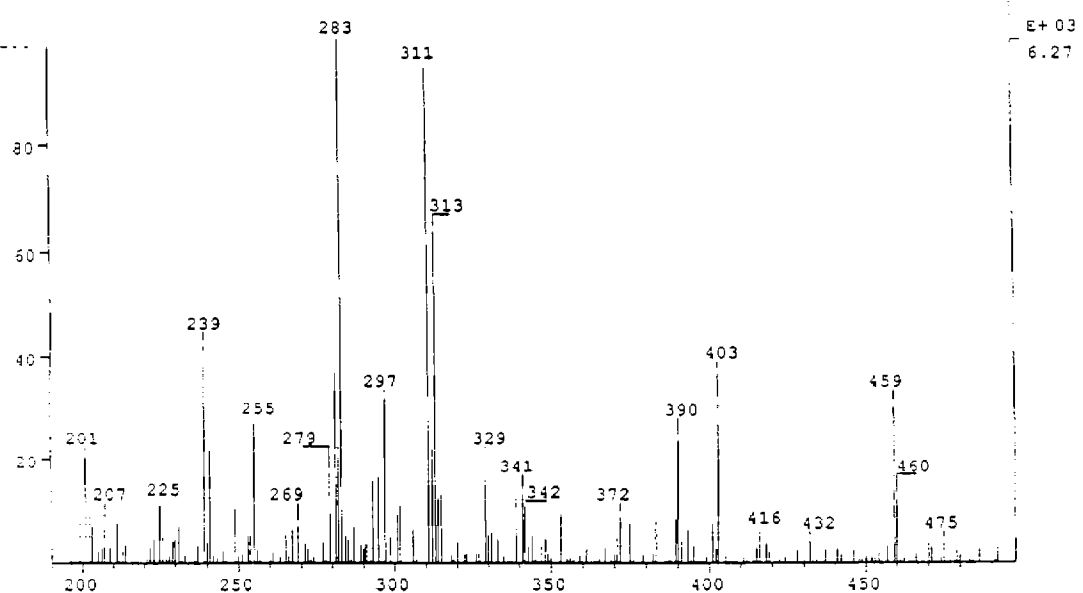


FIGURE 17. THERMOSPRAY/MS OF COMPONENT 3B

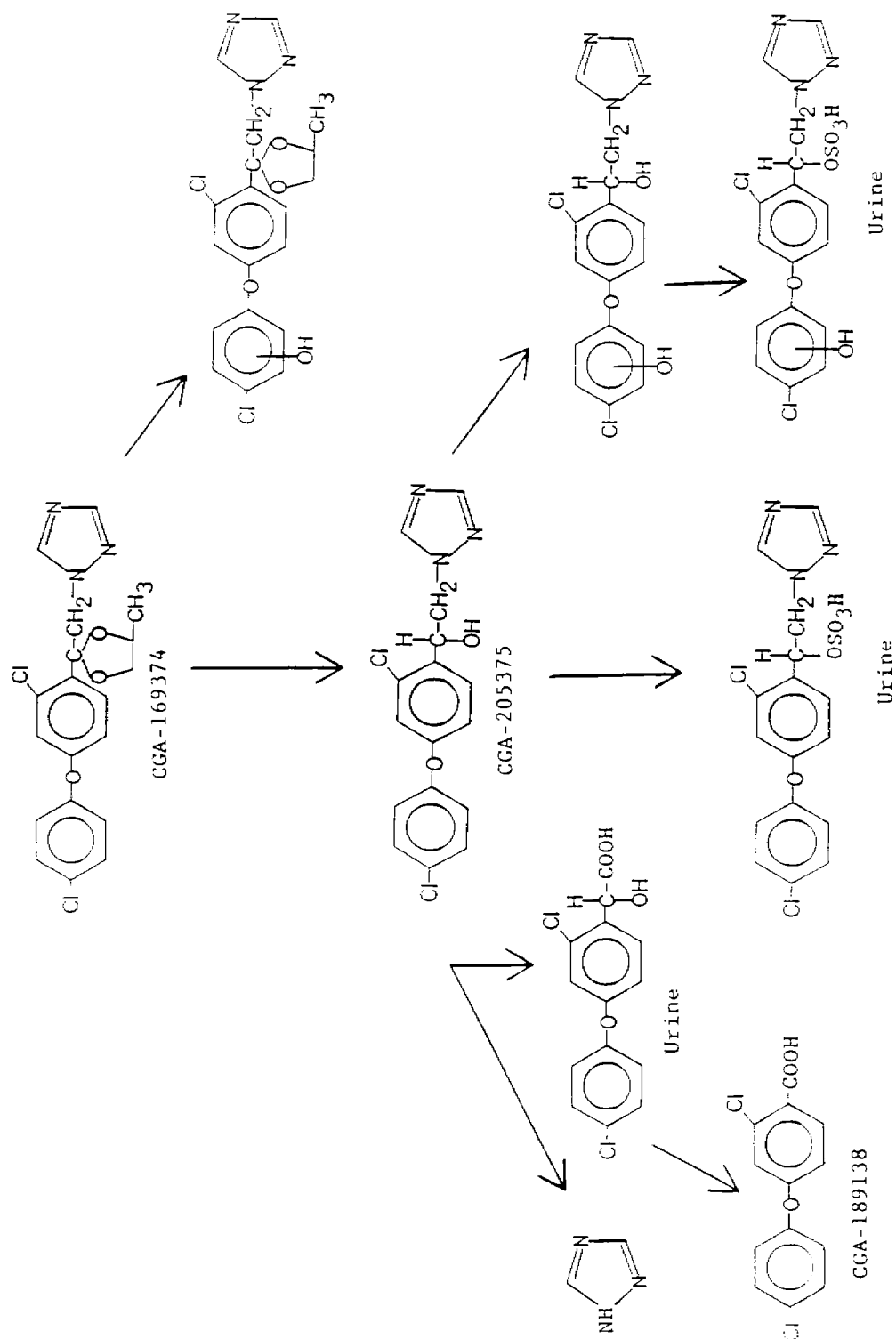


FIGURE 18. METABOLIC PATHWAY OF CGA-169374 IN RATS

IX. REFERENCES

1. Protocol Number 98-86, "Metabolism of Phenyl-¹⁴C-CGA-169374 in the Rat."
2. Protocol Number 99-86, "Metabolism of Triazole-¹⁴C-CGA-169374 in the Rat."
3. Barr, H. P., Capps, T. M. and Carlin, T. J., ABR-90019, "Characterization and Identification of Major Triazole-¹⁴C and Phenyl-¹⁴C-CGA-169374 Metabolites in Rats."
4. Capps, T. M., Cassidy, J. E. and McFarland, J. E., ABR-88043, "Metabolism of Triazole-¹⁴C and Phenyl-¹⁴C-CGA-169374 in the Rat - Distribution of Radioactivity."